FAILURE OF PRECRACKED FIBER REINFORCED COMPOSITE PLATE

Thesis by

Narayan K. Mahale

In Partial Fulfillment of the Requirements

For the Degree of

Aeronautical Engineer

California Institute of Technology

Pasadena, California

1973

(Submitted, September 22, 1972)

ACKNOWLEDGEMENTS

The author is grateful to Dr. W. G. Knauss and Dr. C. D. Babcock for their guidance during all phases of the work for this thesis. Credit for the experiments on the measurement of the elastic constants by the method of cantilever vibration goes to Mr. Ahmet Ozkul. The help given by Mr. W. A. Rae during various experimental stages is highly appreciated. The author is very thankful to Mrs. Elsa Titchenell, Miss Helen Burrus, Mrs. Connie Peterson and Mrs. Virginia Conner for typing the thesis. The material was made available through the courtesy of Dr. E. L. Harmon of the Aircraft Division of the Northrop Corporation. Thanks is also due to Mrs. Betty Wood for drawing the figures.

ABSTRACT

In the following pages a theoretical and experimental investigation of the fracture of a precracked carbon fiber reinforced composite is presented. The work deals mainly with a unidirectional composite having the crack aligned parallel to the fibers. We put forth some ideas on how to extend the failure criterion of the above restricted case to a more general one of multidirectional composites. The failure criterion proposed is based on an energy argument similar to that proposed by Griffith for isotropic solids. For the purpose of stress analysis the material under consideration is assumed to be homogeneous and orthotropic. Lekhnitskii's complex variable method of stress analysis of the two dimensional elasticity problems for anisotropic bodies is used in the theoretical investigation.

TABLE OF CONTENTS

LIST OF FIGURES

LIST OF TABLES

LIST OF SYMBOLS

a	half crack length
E_{xx}, E_{yy}	Young's moduli of orthotropic material along the axis of symmetry
G_{xy}	corresponding shear modulus
i	$\sqrt{-1}$
K_I	stress intensity factor for the normal mode
K_{II}	stress intensity factor for the shear mode
K_{Ic}, K_{IIc}	corresponding critical stress intensity factors
U	work done by the tractions during opening of the crack
U_I	work done by the normal traction
U_{II}	work done by the shear traction
u_i	displacement components
u_x, u	displacement along x axis
u_y, v	displacement along y axis
Z, Z_i	complex variables
x, y, z	cartesian coordinates
ϵ_{ij}	strains
Γ	fracture energy/sq. inch
Γ_o	delamination energy/sq. inch
ν	Poisson's ratio
σ_{ij}	stresses

1. INTRODUCTION

The primary advantages which advanced composites have over conventional engineering metals is that the strength to weight ratio is significantly higher for the former than for the latter. In spite of their extremely high cost this advantage still makes these materials attractive for designs where high strength is required with a minimum of weight. For this reason advanced composite materials find applications in aircraft and space structures. Along with these advantages with regard to the strength come several secondary advantages, which make the use of these materials desirable. One of these advantages deals with the fact that material can be tailored to particular design geometries in such a way that the strength capabilities are exploited to the fullest. Thus, the use of advanced composites can incorporate some optimization in structural design due to material lay-up during manufacturing. It is possible to control the thermal expansion coefficient of the composite by judicious geometrical lay-up. In some cases only the bending flexibility of the material may be decreased without much effect in the bending strength.

On a macroscopic scale advanced composites are treatable as more or less homogeneous anisotropic solids (1, 2, 3). However, on a microscopic scale these materials are inhomogeneous. The failure of advanced composites, in the form of fracture, is intimately connected with the growth of microscopic flaws which one finds invariably embedded in the inhomogeneous structure of the material. The growth of these microscopic flaws under the applied load is therefore also governed by the small scale geometry of the composites and it is

readily appreciated that the growth of such flaws through the inhomogeneous structure of composites constitutes a formidable problem for the analyst. It goes, therefore, without saying that the detailed treatment of fracture of composites is a difficult problem at best, and one is readily led to deal with the approximate characterization of the failure properties.

The fiber reinforced composite consists of units of construction called plys -- the ply is a layer of fibers, vacuum deposited wires of boron or drawn glass wires or threads of graphite, impregnated with a resin -- several of which are laid-up to obtain a sheet of required thickness. The composite material containing plys with the fibers oriented in the same direction is a unidirectional composite. If the fibers of different plys are oriented at different directions with respect to each other, then the composite is termed a multidirectional composite (fig. 1-1). Before dealing with such more complex problems of failure in multidirectional composites, it is desirable that the fracture behavior of single-ply or unidirectional composites be understood. In the following we shall deal with the behavior of a unidirectional graphite fiber-epoxy matrix composite. This material is an eight-ply sheet about 60 thousandths of an inch thick. The material contains 33.4% resin by weight or 60% fiber by volume. The specific gravity is 1.584. The fibers were produced by Cort-Holes and impregnated by Ferro with the resin Hercules 3002. The sheet was 18" x 20" and was made available through the courtesy of Dr. E. L. Harmon of the Aircraft Division of the Northrop Corporation.

2. PRELIMINARIES

We have already referred to the fact that a fiber-reinforced composite, on a microscopic scale, is inhomogeneous. Continuum analyses for an anisotropic body are available only for the homogenously anisotropic solids. The use of such a theory therefore restricts us to consider such geometries involving crack sizes which are large compared to the structural inhomogeneities of the solids, such that we may at least approximately deal with the solids on a macroscopically homogeneous scale. Such treatments are apparently generally accepted when one deals with analyses of advanced composites (1,2,3).

Wu (3) has postulated an empirical failure criterion. He compares stress distribution in isotropic and anisotropic bodies, and in both cases, the same order of singularities exists. Let σ and τ be the normal and shear stresses and c the half crack length. Then the stress intensity factors $K_I = \sigma\sqrt{c}$ and $K_{II} = \tau\sqrt{c}$ can be defined. K_{Ic} and K_{IIc} are, respectively, the critical stress intensity factors under normal and shear loads. Then the equation (2.1) is assumed to be a failure criterion on the basis of dimensional analysis, where m and n are

$$\left(\frac{K_I}{K_{Ic}}\right)^m + \left(\frac{K_{II}}{K_{IIc}}\right)^n = 1 \qquad (2.1)$$

empirical factors chosen to the best agreement with experimental results. From the pure tension ($\tau = 0$) and pure shear ($\sigma = 0$) tests K_{Ic} and K_{IIc} are evaluated. Further experiments for the case of various combinations of tension and shear were used to determine m and n, which were found to be about 1 and 2 respectively. Experiments were conducted with Balsa Wood (3) as well as fiber-glass-epoxy

(2) to check the proposed relation, (eq. 2.1). McKinney (4) performed some experiments on the graphite-epoxy composite and fitted, by a least square technique, equation (2.1) to his data, and he found results identical with those obtained by Wu.

Stonesiefer and Sanford (1) have experimented on the double and single notched specimen to determine the failure criterion. They argued that the energy release rate through crack propagation is independent of mode of loading and thus suggested that one parameter of energy release rate in the opening mode is sufficient to characterize the fracture under arbitrary loading conditions.

In the work of these past references, it was normally observed that the crack propagates parallel to the fibers. This is not unreasonable at all. The fibers used are of considerably high strength compared to the strength of the matrix. The crack requires less release of strain energy when it propagates through the matrix than when it propagates across the fibers. Thus failure is much more likely to occur through the matrix. In polylayered composites a crack will tend to propagate in the direction of the fibers in each ply. But the crack will not be able to travel too long a distance in any one layer before the stresses at the propagating tip are alleviated due to the restraining influence of the adjacent layers. Fracture of the multiple crack tip will not be accomplished until the crack in the individual plys are joined up through the interlaminar layers. It may thus be possible to synthesize a conservative estimate of crack propagation in multilayered composites by considering what happens to the cracks in individual layers and from the energy requirements that are necessary to join

up these crack extensions. This problem will be considered in section 4.

We first consider the problem of a unidirectional composite plate, ideally of infinite extent, in which is embedded a rectilinear crack of specified size 2a (fig. 2-1), parallel to the fibers and tension is applied at infinity at some angle φ (fig. 2-1), the tension at infinity being uniform and of value P. Since our intention is to study this problem experimentally for the determination of realistic material parameters, it is necessary to deal with finite specimens. The fact that the cost of the material is high induces us to deal with a minimum size specimen. If we deal with relatively small sizes, it is necessary that we know that the stress distribution in the small specimen is sufficiently well approximated by the solution for an infinite plate. Our first aim is therefore to calculate those sizes of the specimen with a predetermined crack, which allow a reasonable approximation to the infinite sheet. It was decided to determine the sizes of rectangular specimens, such that the stresses on the boundaries are within 5% of the uniform far field stresses for the infinite sheet. The displacements on these boundaries were also calculated. The specimens were made slightly larger to account for mounting the tension device (See section 6).

This report will be presented in the following sections: First, we shall deal with the stress analyses and sizing of the specimen. Next, the formulation of a failure criterion for unidirectional composites will be presented with a brief sketch of the syntheses of a conservative estimate for multidirectional composites. We then deal with the determination of the elastic properties in Section 5, and discuss the experimental set-up in the next section. The last section will deal with the experimental results and their analysis.

3. STRESS ANALYSIS

A. Review of the Stress Analysis of an Infinite Plate Containing a Finite Rectilinear Crack.

We shall now present an outline for the stress analysis of an infinite orthotropic plate containing a crack. We consider the case where the body forces are absent and the stresses are only due to far field tension. We shall consider this as one of generalized plane stress.

As the equilibrium equations are independent of the constitutive relation of the material, we have for the planar problem, x and y being in the plane of the plate,

$$\left.\begin{aligned} \frac{\partial \sigma_{xx}}{\partial x} + \frac{\partial \sigma_{xy}}{\partial y} &= 0 \\ \frac{\partial \sigma_{xy}}{\partial_x} + \frac{\partial \sigma_{yy}}{\partial y} &= 0 \end{aligned}\right\} \tag{3.1}$$

Similarly the analysis of strain leads to the reduction of the set of compatibility equations, as in the isotropic case, to a single compatibility equation, namely,

$$\frac{\partial^2 \epsilon_{yy}}{\partial x^2} + \frac{\partial^2 \epsilon_{xx}}{\partial y^2} = \frac{2\partial^2 \epsilon_{xy}}{\partial_x \partial_y} \tag{3.2}$$

With regard to the constitutive relation of an orthotropic planar body,

we note that axes of orthotropy constitute a natural reference frame. With respect to such a coordinate system, we write the constitutive relation in the form,

$$\begin{bmatrix} \epsilon_{xx} \\ \epsilon_{yy} \\ 2\,\epsilon_{xy} \end{bmatrix} = \begin{bmatrix} \frac{1}{E_{xx}} & -\frac{\nu_{xy}}{E_{xx}} & 0 \\ -\frac{\nu_{yx}}{E_{yy}} & \frac{1}{E_{yy}} & 0 \\ 0 & 0 & \frac{1}{G_{xy}} \end{bmatrix} \begin{bmatrix} \sigma_{xx} \\ \sigma_{yy} \\ \sigma_{xy} \end{bmatrix} \tag{3.3}$$

where,
$$\frac{\nu_{xy}}{E_{xx}} = \frac{\nu_{yx}}{E_{yy}} \tag{3.4}$$

We now choose a stress function $\chi(x, y)$ (ref. 2) defined by differential relation,

$$\begin{aligned} \sigma_{xx} &= \chi_{yy} \\ \sigma_{yy} &= \chi_{xx} \\ \sigma_{xy} &= \chi_{xy} \end{aligned} \tag{3.5}$$

such that the stresses σ_{xx}, σ_{yy} and σ_{xy} satisfy the equilibrium equations identically. Using the constitutive relation (3.4) to express the strains ϵ_{ij} in terms of the stresses σ_{ij}, and substituting the strain thus obtained, into the compatibility equation (3.2), by virtue of (3.5), leads to a fourth order partial differential equation in terms of the stress function χ,

$$\chi_{xxxx} + 2A\chi_{xxyy} + B\chi_{yyyy} = 0 \tag{3.6}$$

where the constants A and B are,

$$A = \frac{E_{xx}}{2G_{xy}} - \nu_{xy} \qquad B = \frac{\nu_{xy}}{\nu_{yx}}$$

Let us define the operator D_K by the expression,

$$D_K = \frac{\partial}{\partial_x} - \mu_K \frac{\partial}{\partial_y} \tag{3.7}$$

where μ_K is the appropriately chosen complex constant (ref. 5, p. 120). It can be verified by substitution that the quadruple operational equation

$$D_1 D_2 D_3 D_4 \chi = 0 \tag{3.8}$$

is equivalent to the partial differential equation (3.7), provided the constants A and B are identified as suitable combinations of the constants μ_K, K = 1, 2, 3, 4. The solution to the equation (3.8) is (ref. 5, p. 122),

$$\chi = \sum_{1}^{4} F_K (x + \mu_K y) \tag{3.9}$$

where $F_K(x + \mu_K)$ are the functions of the argument $x + \mu_K y$, and the solution of the differential equations

$$D_K F_K (x + \mu_K y) = 0 \tag{3.10}$$

If $Z_1 = x + \mu_1 y$ and $Z_2 = x + \mu_2 y$ are used as complex variables, since μ_K are complex, the solution to (3.8) can be written

(ref. 2 pp. 122-123)

$$\chi = 2\mathcal{R}e\left[F_1(Z_1) + F_2(Z_2)\right] \tag{3.11}$$

Now let us write

$$\Phi_K = F_K'(Z_K) = \frac{\partial F_K(Z_K)}{\partial Z_K} \tag{3.12}$$

In the present case when x and y are the axes of orthotropy, we find that μ_1 and μ_2 are imaginary and it is convenient to write $\mu_1 = i s_1$ and $\mu_2 = i s_2$ where,

$$s_1 = \sqrt{\left(\frac{E_{xx}}{2G_{xy}} - \nu_{xy}\right) + \sqrt{\left(\frac{E_{xx}}{2G_{xy}} - \nu_{xy}\right)^2 - \frac{E_{xx}}{E_{yy}}}}$$

$$s_2 = \sqrt{\left(\frac{E_{xx}}{2G_{xy}} - \nu_{xy}\right) - \sqrt{\left(\frac{E_{xx}}{2G_{xy}} - \nu_{xy}\right)^2 - \frac{E_{xx}}{E_{yy}}}} \tag{3.13}$$

Then we can write the stresses σ_{ij}, and the displacements u; as (ref. 5, p. 137)

$$\left.\begin{aligned} \sigma_{xx} &= -2\mathcal{R}e\left[s_1^2 \Phi_1'(Z_1) + s_2^2 \Phi_2'(Z_2)\right] \\ \sigma_{yy} &= 2\mathcal{R}e\left[\Phi_1'(Z_1) + \Phi_2(Z_2)\right] \\ \sigma_{xy} &= -2\mathcal{R}e\left[i s_1 \Phi_1'(Z_1) + i s_2 \Phi_2'(Z_2)\right] \end{aligned}\right\} \tag{3.14}$$

$$\left.\begin{aligned} u_x = u &= 2\mathcal{R}e\left[\rho_1 \Phi_1(Z_1) + \rho_2 \Phi_2^1(Z_2)\right] \\ u_y = v &= 2\mathcal{R}e\left[q_1 \Phi_1(Z_1) + q_2 \Phi_2^1(Z_2)\right] \end{aligned}\right\} \tag{3.15}$$

where

$$\rho_1 = -\frac{s_1^2}{E_{xx}} - \frac{2\nu_{xy}}{E_{xx}}$$

$$\rho_2 = -\frac{s_2^2}{E_{yy}} - \frac{2\nu_{yx}}{E_{yy}}$$

$$q_1 = i\,\frac{\nu_{yx} s_1^2}{E_{yy}} + \frac{1}{E_{yy}} \qquad (3.16)$$

$$q_2 = i\,\frac{\nu_{yx} s_2^2}{E_{yy}} + \frac{1}{E_{yy}}$$

We have now determined the stress function χ in terms of the unknown functions $\Phi_1(Z_1)$ and $\Phi_2(Z_2)$. We have to determine these functions in such a manner that the boundary conditions for our particular problem are satisfied.

We are interested in obtaining the stresses in the vicinity of a crack embedded in an infinite sheet. As the crack is a limiting case of an ellipse as the minor axis approaches zero, we wish to start by considering an infinite plate perforated with an elliptic hole, the major axis being 2a and the minor axis 2b (fig. 3-1), uniform tension P being applied at infinity at an angle φ (fig. 3-1) with respect to the major axis.

We superpose two problems to obtain the solution to the desired problem. First we consider a plate under uniform tension without a perforation. Secondly, we consider a plate with an elliptic hole, on the periphery of which we prescribe the tractions which are opposite

to those found on the hypothetical ellipse boundary of the non-perforated plate in the first problem. When the two problems are superposed (added), we find that the stresses at infinity and on the boundary of the ellipse are as required in the original problem. Let σ_{xx}^{o}, σ_{yy}^{o} and σ_{xy}^{o} be stresses in the plate when the hole is absent and σ_{xx}^{1}, σ_{yy}^{1} and σ_{xy}^{1} be stresses for the second problem. The final solution then will be the addition of the two stress states and is given by,

$$\left.\begin{aligned} \sigma_{xx} &= \sigma_{xx}^{o} + \sigma_{xx}^{1} \\ \sigma_{yy} &= \sigma_{yy}^{o} + \sigma_{yy}^{1} \\ \sigma_{xy} &= \sigma_{xy}^{o} + \sigma_{xy}^{1} \end{aligned}\right\} \qquad (3.17)$$

The solution to the first problem is trivial and is,

$$\left.\begin{aligned} \sigma_{xx}^{o} &= P\cos^{2}\varphi \\ \sigma_{yy}^{o} &= P\sin^{2}\varphi \\ \sigma_{xy}^{o} &= P\sin\varphi\cos\varphi \end{aligned}\right\} \qquad (3.18)$$

The solution of the second problem is somewhat complicated and we will follow Lekhnitskii's development (ref. 5, p. 158); accordingly we take $\Phi_1(Z_1)$ and $\Phi_2(Z_2)$ as

$$\left.\begin{aligned} \Phi_1(Z_1) &= A_1 \ell n\, \zeta_1 + \frac{1}{\mu_1-\mu_2}\sum_{1}^{\infty}(\bar{b}_m - \mu_2\bar{a}_m)\,\zeta_1^{-m} \\ \Phi_2(Z_2) &= A_2 \ell n\, \zeta_2 + \frac{1}{\mu_2-\mu_1}\sum_{1}^{\infty}(\bar{b}_m - \mu_1\bar{a}_m)\,\zeta_2^{-1} \end{aligned}\right\} \qquad (3.19)$$

where,

$$\zeta_1 = \frac{Z_1 + \sqrt{Z_1^2 - a^2 - \mu_1^2 b^2}}{a - i\mu_1 b} \quad \text{and } Z_1 = x + \mu_1 y$$

$$\zeta_2 = \frac{Z_2 + \sqrt{Z_2^2 - a^2 - \mu_2^2 b^2}}{a - i\mu_2 b} \quad \text{and } Z_2 = x + \mu_2 y$$

For the case of uniform tension at infinity (ref. 2, p. 158), we have,

$$A_1 = A_2 = 0$$

$$\bar{a}_m = \bar{b}_m = 0 \qquad m \geq 2 \tag{3.20}$$

and

$$\bar{a}_1 = \frac{P}{2} \sin\varphi \left[a \sin\varphi - i b \cos\varphi \right]$$

$$\bar{b}_1 = \frac{P}{2} \cos\varphi \left[a \sin\varphi - i b \cos\varphi \right] \tag{3.20}$$

Recalling that a and b are respectively the semimajor and semiminor axes of the ellipse, we pass to the solution for the stresses in the vicinity of the crack by allowing b to approach zero. It follows that the Φ_1 and Φ_2 reduce to,

$$\Phi_1(Z_1) = \frac{Pa^2 \sin\varphi}{2i(s_1 - s_2)} (\cos\varphi + i s_2 \sin\varphi) \frac{1}{Z_1 + \sqrt{Z_1^2 - a^2}}$$

$$\Phi_2(Z_2) = -\frac{Pa^2 \sin\varphi}{2i(s_1 - s_2)} (\cos\varphi + i s_1 \sin\varphi) \frac{1}{Z_2 + \sqrt{Z_2^2 - a^2}} \tag{3.21}$$

Recall again that Φ_1 and Φ_2 give the solution to the second problem stated above for the infinite plate containing an elliptic perfora-

tion, on the boundary of which certain tractions are prescribed. In order to obtain the expressions for the stresses and displacements in the second problem we substitute $\Phi_1(Z_1)$ and $\Phi_2(Z_2)$ in equations (3.14) and (3.15) respectively, to obtain

$$\sigma_{xx} = \frac{P a^2 \sin^2\varphi}{s_1 - s_2} \operatorname{Re}\left\{ \frac{i s_1^2(\cos\varphi + i s_2 \sin\varphi)}{(Z_1^2 - a^2)^{\frac{1}{2}}(Z_1 + \sqrt{Z_1^2 - a^2})} - \frac{i s_2^2(\cos\varphi + i s_1 \sin\varphi)}{(Z_2^2 - a^2)^{\frac{1}{2}}(Z_2 + \sqrt{Z_2^2 - a^2})} \right\}$$

$$\sigma_{yy} = \frac{P a^2 \sin^2\varphi}{s_1 - s_2} \operatorname{Re}\left\{ \frac{i(\cos\varphi + i s_2 \sin\varphi)}{(Z_1^2 - a^2)^{\frac{1}{2}}(Z_1 + \sqrt{Z_1^2 - a^2})} - \frac{i(\cos\varphi + i s_i \sin\varphi)}{(Z_2^2 - a^2)^{\frac{1}{2}}(Z_2 + \sqrt{Z_2^2 - a^2})} \right\}$$

$$\sigma_{xy} = \frac{P a^2 \sin^2\varphi}{s_1 - s_2} \operatorname{Re}\left\{ \frac{s_1(\cos\varphi + i s_2 \sin\varphi)}{(Z_1^2 - a^2)^{\frac{1}{2}}(Z_2 + \sqrt{Z_2^2 - a^2})} - \frac{s_2(\cos\varphi + i s_1 \sin\varphi)}{(Z_1^2 - a^2)^{\frac{1}{2}}(Z_2 + \sqrt{Z_2^2 - a^2})} \right\} \quad (3.23a)$$

$$u = -\frac{P a^2 \sin\varphi}{s_1 - s_2} \operatorname{Re}\left\{ \frac{i p_1 (\cos\varphi + i s_2 \sin\varphi)}{Z_1 + \sqrt{Z_1^2 - a^2}} - \frac{i p_2 (\cos\varphi + i s_1 \sin\varphi)}{Z_2 + \sqrt{Z_2^2 - a^2}} \right\}$$

$$v = +\frac{P a^2 \sin\varphi}{s_1 - s_2} \operatorname{Re}\left\{ \frac{i q_1 (\cos\varphi + i s_2 \sin\varphi)}{Z_1 + \sqrt{Z_1^2 - a^2}} - \frac{i q_2 (\cos\varphi + i s_1 \sin\varphi)}{Z_2 + \sqrt{Z_2^2 - a^2}} \right\} \qquad (3.23b)$$

B. Considerations on the Singular Stress Distribution

We note that the stresses expressed in equation (3.22) behave in singular fashion as the point under consideration approaches the crack tip. From a physical viewpoint such behavior is not admissible since no material can withstand infinite stresses. We comment, not as an excuse, but as a point of information that the singular stresses are obtained also in an isotropic solid. The mechanics of fracture in an isotropic solid has assumed the results of the classical theory of linear elasticity, in spite of the presence of the singular stresses, to predict the fracture behavior of homogeneous isotropic solids. The saving grace in this connection is the fact that the energy contained within the singular part of the stress is finite. This has led Griffith to the formulation of the energy criterion for the fracture. The fact that the energy contained in the singular region is finite, is also true in anisotropic bodies. We shall at a later point proceed to formulate the fracture criterion for an orthtropic plate with a crack, on the same basis as that advanced by Griffith.

Presently we wish to interpret the unrealistic high stresses in terms of a more realistic physical situation, near the crack tip in an anistropic solid. Undoubtedly, microstructurally, the inhomogeneous material becomes nonlinear when large stresses are encountered. For this reason the material at the tip of the crack will no longer respond in a linear fashion as assumed to be the case for the bulk material; instead it will break down, being able to carry a lesser load. As a result, the stress field in the body, in the vicinity of the tip will

change so that these high but finite stresses will act over some domain at the tip so as to satisfy the overall equilibrium. This kind of material has been encountered in connection with plasticity in isotropic bodies (ref. 6). In spite of the small scale nonlinear behavior of the material it has been found in the case of the isotropic bodies that the fracture behavior is reasonably well predicted by the linear elasticity. With such practical experience in mind, we treat the singular behavior in an orthotropic solid in an admittedly somewhat cavalier fashion, overlooking the physical reality of nonlinear behavior of the material at the tip of the crack. Therefore we clearly follow the examples in the fracture of the isotropic solids and apply the linear elastic theory in the fracture mechanics of an anisotropic body.

C. Strain Energy in a Plate due to the Crack

We are interested in the propagation of the crack under far field loading. According to our hypothesis (see section 4), crack propagation takes place if the amount of the strain energy released during the crack propagation is equal to or exceeds the surface energy required to form the new crack surface. Let u_o and v_o be the displacements of the crack surface and let σ_{yyo}^{1} and σ_{xyo}^{1} be the tractions acting on the crack surface, U_I be the work done by the normal tractions σ_{yyo}^{1} and U_{II} be the work done by the shear tractions σ_{xyo}^{1}. U_I and U_{II} are given by

$$
\begin{aligned}
U_I &= \frac{1}{2}\left[2\int_{-a}^{a} \sigma_{yyo}^{1}\, v_o \, dx\right] \\
&= \frac{\pi}{2}\,\frac{(s_1+s_2)\,P^2 a^2 \sin^2\varphi}{E_{yy}} \\
U_{II} &= \frac{1}{2}\left[2\int_{-a}^{a} \sigma_{xyo}^{1}\, u_o \, dx\right] \\
&= \frac{\pi}{2}\,\frac{(s_1+s_2)a^2P^2\sin^2\varphi\cos^2\varphi}{\sqrt{E_{xx}E_{yy}}}
\end{aligned}
\qquad (3.23)
$$

For the total work U, done by tractions Ti we have

$$
\begin{aligned}
U &= \frac{1}{2}\left[2\int_{-a}^{a} u_i\, Ti\, dx\right] \\
&= \frac{1}{2}\left[2\int_{-a}^{a} v_o\, \sigma^{1}_{xyo}\, dx + 2\int_{-a}^{a} u_o\, \sigma_{yyo}\, dx\right] \\
&= U_I + U_{II}
\end{aligned}
\qquad (3.24)
$$

Hence we have from equations (3.23) and (3.24),

$$U = \frac{1}{2} \frac{(s_1+s_2)a^2}{\sqrt{E_{yy}}} \left[\frac{P^2 \sin^4\varphi}{\sqrt{E_{yy}}} + \frac{P^2 \cos^2\varphi \sin^2\varphi}{\sqrt{E_{xx}}} \right]$$

$$= \frac{1}{2} \frac{(s_1+s_2)a^2}{\sqrt{E_{yy}}} \left[\frac{\sigma_{yy}^{o\,2}}{\sqrt{E_{yy}}} + \frac{\sigma_{xy}^{o\,2}}{\sqrt{E_{xx}}} \right] \qquad (3.25)$$

We note parenthetically that for the isotropic case, $s_1 = s_2 = 1$ and $E_{xx} = E_{yy} = E$, so that one obtains

$$= \frac{a^2}{E} \left(\sigma_{yy}^{o\,2} + \sigma_{xx}^{o\,2} \right) \qquad (3.26)$$

This same expression is obtained for the isotropic plate with a rectilinear crack, under same loading conditions as above (6).

4. Theoretical Failure Criterion

A. Stability Criterion

Consider a plate of fiber composite material containing a crack, loaded in tension of magnitude P as indicated earlier and depicted in (fig. 2.1), the crack being oriented parallel to the fibers. Without further defining the meaning of weak or strong, we refer to an earlier statement, in which we had characterized the matrix as weak when compared to the fibers. We point out however, that the fibers are intrinsically stronger only in tension along their axis, whereas they may come apart, "relatively easily" if the tension were applied normal to the draw direction. We make this statement because we do not want to infer that the intrinsic weakness of composite materials transverse to the fibers derives from the weakness of the matrix but it could equally well derive from the weak transverse strength characteristics of the fibers. It appears intuitively obvious to us that the crack requires much less energy if it propagates parallel to the fibers than if it were to grow so that it would rupture the fibers. But if the crack is almost aligned with the direction of tension it may well be possible that the tension required to propagate the crack parallel to the fibers may exceed the tension required to propagate the crack transverse to them. We expect that this would occur when φ (fig. 2.1) is a few degrees. Our present aim is to investigate the cases when the crack propagates along the fibers. We leave for the later investigation the cases when the crack transgresses the fibers.

Next we associate with the propagation of the crack parallel to the fibers a definite surface energy requirement and we assume that for

a unit of new fracture surface generated an amount of energy Γ is required. Simultaneously with this assumption we advance a corollary supposition that neither the matrix material nor the fiber material undergoes plastic deformation and that the material stays elastic and brittle. This supposition primarily is a matter of convenience rather than of a physical reality. But in view of the brittle properties of the matrix material and the fiber material we expect this assumption to be not of adverse consequences.

The assumption regarding the development of a stability criterion - viz: that the crack moves parallel to the fibers - is contingent on the further assumption that the matrix volume fraction is small. We illustrate this point by considering what might happen if the matrix volume fraction is large. In this case a crack, located parallel to the fibers and subjected to the normal as well as the shear stresses, would propagate at some angle to its original orientation (fig. 4.1), until it encounters the fibers. Near the fibers the stress field will be three dimensional and the manner in which the crack grows will not be along the fibers. Theoretical determination of the stress field is impossible. Due to the irregularities in fibers the actual path will also be irregular. However the surface area thus generated will not be planar, and the assumption of the colinear crack propagation will not be justified. We therefore assume implicitly that the fiber volume is large compared to the matrix volume such that distance between the surfaces of adjucent fibers is small, compared to the fiber diameter. This assumption is justified when the fibers occupy 60% of the composite volume.

In order to determine the stability of the crack in an orthotropic plate we consider a virtual enlargement of the crack and examine the effect of this virtual growth on the stored energy as a function of crack extension. In order to do this we consider first the energy stored in the plate, containing a crack of length 2a , and secondly consider the energy in the plate containing a crack of length 2 (a + Δa). In view of the resulting equation (3.25), the work done by the tractions against the moving boundary of the crack of length 2a, is,

$$U(a) = \frac{\pi}{2} \frac{(s_1 + s_2)\, a^2}{\sqrt{E_{yy}}} \left[\frac{\sigma_{yy}^{o}}{\sqrt{E_{yy}}} + \frac{\sigma_{xy}^{o}}{\sqrt{E_{xx}}} \right] \tag{4.1}$$

while the work done by the traction against the moving boundary of the crack of length 2 (a + Δa) is,

$$U(a) = \frac{\pi}{2} \frac{(s_1 + s_2)\, (a+\Delta a)^2}{\sqrt{E_{yy}}} \left[\frac{\sigma^{o}_{yy}}{\sqrt{E_{yy}}} + \frac{\sigma^{o}_{xy}}{\sqrt{E_{xx}}} \right] \tag{4.2}$$

Now, we find the amount of strain energy available to do the work against the surface energy, by finding the difference between the case of crack length 2a and the case of crack length 2 (a + Δa). Next form the ratio of the difference of the strain energy to the crack enlargement Δa, then pass to the limit as Δa approaches zero. The result is,

$$\lim_{\Delta a \to 0} \frac{\Delta U}{\Delta a} = \frac{dU}{da} = \frac{\pi (s_1 + s_2)\, a}{\sqrt{E_{yy}}} \left(\frac{\sigma_{yy}^{o\,2}}{\sqrt{E_{yy}}} + \frac{\sigma_{xy}^{o\,2}}{\sqrt{E_{xx}}} \right) \tag{4.3}$$

In the process of enlarging the crack length by Δa on either side of the crack tips, surface energy in the amount of $4\Gamma\Delta a$ is required. This surface energy is equal to the available strain energy release

(4.3) at the point of instability. We thus obtain,

$$4\Gamma \Delta a = \frac{dU}{da} \Delta a \tag{4.4}$$

Substituting $\frac{dU}{da}$ from (4.3) into (4.4) we get,

$$4\Gamma = \frac{\pi (s_1+s_2)^a}{\sqrt{E_{yy}}} \left(\frac{\sigma_{yy}^{o2}}{\sqrt{E_{yy}}} + \frac{\sigma_{xy}^{o2}}{\sqrt{E_{xx}}} \right) \tag{4.5}$$

The stress intensity factors K_I and K_{II} are defined as,

$$\sigma_{ij} = \frac{K}{\sqrt{2\pi r}} f(\theta) \tag{4.6}$$

In our case this leads to,

$$K_I = \sigma_{yy}^{o} \sqrt{a} \quad \text{and} \quad K_{II} = \sigma_{xy}^{o} \sqrt{a} \tag{4.7a}$$

Let us further define the material constants α and β as,

$$\alpha = \frac{4\Gamma E_{yy}}{\pi(s_1+s_2)} \qquad \beta = \frac{4\Gamma \sqrt{E_{xx}E_{yy}}}{\pi (s_1+s_2)} \tag{4.7b}$$

By virtue of (4.7a), (4.7b), equation (4.5) then reads,

$$\left(\frac{K_I}{\alpha}\right)^2 + \left(\frac{K_{II}}{\beta}\right)^2 = 1 \tag{4.8}$$

We now assert that the relation (4.8) should be satisfied at the point of incipient crack propagation, with propagation parallel to the fibers, under arbitrary loading conditions except when φ (fig. 3.1) is small.

B. Comparison With Wu's Criterion

As mentioned in (Section 2) Sanford and Stonsiefer's work is in close accord with the present development. However Wu's empirical criterion is significantly different and deserves some further comments.

As pointed out in (Section 2), Wu assumes, on the basis of dimensional analysis, that the failure relation is given by equation (2.1), repeated here for convenience,

$$\left(\frac{K_I}{K_{Ic}}\right)^m + \left(\frac{K_{II}}{K_{IIc}}\right)^n = 1 \qquad (2.1)$$

where, K_{Ic}, K_{IIc}, m and n are to be determined experimentally. Wu determined K_{Ic} and K_{IIc}, respectively by tension normal to the crack and by pure shear in which the crack is parallel to the shear direction; m and n were then deduced from further experiments under combined loading. The values for m and n were found to be 1.03 and 1.88 respectively, for the experiments on balsa wood. Wu then argued on physical grounds that the power n=1.88 and m=1.03 should be n=2 and m=1 and such values should be obtainable with better experiments. We note, however, that the value of m as predicted experimentally by Wu is unity while in the present theory it takes the value two. We are now faced with the problem of explaining the difference.

The argument given by Wu in order to accept the value of n=2 is, that the sign of the shear should be of no consequence in the failure criterion. This is correct; and one is thus lead to the fact that n should be even; since the experimentally determined value is 1.8, the nearest even number is 2.

Next Wu argues that the value of m=1.03 should be unity. The reasoning used by Wu as to the choice of m=1 is fallacious. It is based on the implicitly assumed existence of a negative stress intensity factor K_I where the crack faces are pressed together; this has no singular solution, and thus a value of K_I does not exist if the crack faces are in uniform contact under pressure.

Let us consider the methods Wu used to determine K_{Ic} and K_{IIc}. The tension experiments for K_{Ic} are adequate. In the case of pure shear experiment this is not necessarily so. In the ideal situation under pure shear testing the crack surfaces will be just in contact without any pressure. However, if the surfaces are not smooth as in the idealized case, but are either slightly serrated or rough because of the inhomogeneities of the material or possibly because of the way the crack was introduced, then there will be apparent friction between the crack surfaces which opposes the enlargement of the crack. Thus the value determined for K_{IIc} will be too large. We now plot both the fracture criterion given by equation (4.8) and Wu's result on the same plot, shown in (fig. 4.2). We notice the the discrepancy arises primarily for the small value of K_I, on which is superimposed Wu's data, in (fig. 4.2), one would observe that all the experimental points follow equally well the equation (4.8) or equation (2.1), except for the points for which K_I=O. However we have already noted that these values for K_{IIc} (K_{Ic}=0) may be high because of the potential inaccuracy of the generation of the smooth fracture surface free of friction. It appears to us, therefore, that the apparently large discrepancy in failure criterion, proposed here and that by Wu, that one exponent

differs by the factor of two may be an artifact of a limited set of experimental points.

C. Extension of the Energy Criterion of Failure to Multidirectional Fiber Composites

It will be recalled that the current study of crack propagation in the unidirectional composite is a precursor to the study of more complex fracture behaviour in multiple layered advanced composite. We find that the detailed consideration of this complex problem is beyond the scope of the present investigation. Let it suffice to put forth some general ideas on how an investigation of this problem should proceed and what might constitute a possibly fruitful avenue, to obtain estimates of fracture bounds in multidirectional composites.

Let us introduce a crack in a composite with multiple oriented fiber layers. The crack will not be aligned with all the fibers but only possibly in a few layers or even only in a single one. As we shall see during the later development the crack will tend to propagate parallel to the fibers. This means that in a multidirectional composite the crack tip attempts to propagate in the direction of the fibers in the different layers. This we expect to hold true if the tension is not aligned very close with the fiber orientation in one or several layers. In view of the supposition a question arises: How far does the crack propagate in the individual layers when the load near the failure point is incremented by small amount? Assuming for the moment that all layers are disconnected, one might argue that the amount of crack propagation in the individual plys for a given time increment is a function of the orientation of the

tension load with respect to the fibers in the individual plys. No estimates exist, as yet, of how much more crack propagation occurs in one ply than in any other one. In predicting, as a first approximation, an upper or a lower bound on the crack propagation in multidirectional composite one might assume equality in all layers. Next we have to contend with the fact that the plys are not disconnected from each other but are connected to each other through the epoxy which is also to be broken in the fracture process, if crack propagation is to occur in individual layer. We envision therefore, that when crack propagation occurs by a small but equal amount in the direction of the fibers in individual plys, a sector-shaped interlaminar region has to be broken in order to allow the crack to propagate in the individual laminates. For example, consider two laminates the orientation of fibers of which is θ with respect to each other. Let the crack tip be located at some point A, the crack having orientations α_1 and α_2 with respect to the two laminae (fig. 4.3). As the crack propagates a distance Δa in either one, the sector of area $(\Delta a)^2 \sin\theta$ has to be broken in a shear deformation mode. The amount of energy required for forming a unit of new surface in shear fracture is Γ_0. The energy required for the shear fracture is then of the order $\Gamma_0 (\Delta a)^2 \sin\theta$. By comparison the amount of energy required for the fracture propagation in individual plys is of the order of $\Delta a \Gamma$ while the energy required to cause the interlaminar failure is of the order $(\Delta a)^2 \Gamma_0$. The question now arises whether the gross failure can be associated with an infinitesimal propagation of the crack in which case the dominant term governing fracture may be that required to begin the propagation in the

individual lamina without consideration of the interlaminar failure provided Γ and Γ_o are of the same order of magnitude. However we may also take a second viewpoint by arguing that the crack propagation in individual laminae is only possible after some local delamination. For example, we may consider that individual laminae permit a small but finite amount of crack extension and that the adjacent layers exert elastic constraint on the further crack propagation, then the crack propagation in each lamina can occur without the gross failure. In that event it is possible that the gross failure of the original crack does not occur until the individual crack extensions of order Δa in each ply have become so large that the dominant failure energy is derived from the interlaminar shear fracture. Then $(\Delta a)^2 \Gamma_o \sin\theta$ may indeed be the controlling factor. The only way in which this can be estimated, it appears to us, is by conducting a series of experiments on specimens with carefully controlled cracks with carefully manufactured multidirectional composites.

To find the load at which the failure in each ply starts we are faced with the task of determining the load shared by each ply. Let us consider a thin plate so that we can assume that strains in each ply are only functions of the in-plane dimensions x and y, the z axis being axis perpendicular to the plate; the strains are same in each ply as well. Let the constitutive equation for the n^{th} layer be,

$$\begin{Bmatrix} \sigma_{xx}^{n} \\ \sigma_{xx}^{n} \\ \sigma_{xx}^{n} \end{Bmatrix} = \begin{bmatrix} a_{11}^{n} & a_{12}^{n} & a_{13}^{n} \\ a_{21}^{n} & a_{22}^{n} & a_{23}^{n} \\ a_{21}^{n} & a_{32}^{n} & a_{33}^{n} \end{bmatrix} \begin{Bmatrix} \epsilon_{xx} \\ \epsilon_{yy} \\ \epsilon_{xy} \end{Bmatrix} \quad (4.9)$$

where the $a^n ij$ are functions of E_{xx}, E_{yy}, G_{xy}, ν_{xy} and angle θ^n between the coordinate system and axis of the ply orthotropy. Let t^n be the thickness of the nth layer. Multiplying 4.9 by t^n and adding over all n's and dividing by the thickness of plate $t = \sum_n t^n$ one obtains,

$$\begin{bmatrix} \frac{\sum_n \sigma^n{}_{xx} t^n}{t} \\ \frac{\sum_n \sigma_{yy}{}^n t^n}{t} \\ \frac{\sum_n \sigma_{xy}{}^n t^n}{t} \end{bmatrix} = \begin{bmatrix} \frac{\sum_n a^n 11\, t^n}{t} & \frac{\sum_n a^n 12\, t^n}{t} & \frac{\sum_n a^n 13 t^n}{t} \\ \frac{\sum_n a_{21}{}^n t^n}{t} & \frac{\sum_n a_{22}{}^n t^n}{t} & \frac{\sum_n a_{23}{}^n t^n}{t} \\ \frac{\sum_n a_{31}{}^n t^n}{t} & \frac{\sum_n a_{32}{}^n t^n}{t} & \frac{\sum_n a^n{}_{33} t^n}{t} \end{bmatrix} \begin{bmatrix} \epsilon_{xx} \\ \epsilon_{yy} \\ \epsilon_{xy} \end{bmatrix} \tag{4.10}$$

Thus the constitutive relation is,

$$\begin{bmatrix} \bar{\sigma}_{xx} \\ \bar{\sigma}_{yy} \\ \bar{\sigma}_{xy} \end{bmatrix} = \begin{bmatrix} \bar{a}_{11} & \bar{a}_{11} & \bar{a}_{13} \\ \bar{a}_{21} & \bar{a}_{22} & \bar{a}_{23} \\ \bar{a}_{31} & \bar{a}_{32} & \bar{a}_{33} \end{bmatrix} \begin{bmatrix} \epsilon_{xx} \\ \epsilon_{yy} \\ \epsilon_{xy} \end{bmatrix} \tag{4.11}$$

where,

$$\frac{\sum_n ai^n j\, t^n}{t} = \bar{a}_{ij}$$

$$\sum_n \sigma_{ij}{}^n t^n = \bar{\sigma}_{ij}$$

Here bar over the quantity denotes the average (elsewhere the bar denotes complex conjugate).

This constitutive law could then be used to determine the average stresses and strains for the cracked plate by Lekhnitskii's method. This information would then enable us to calculate the stresses in the individual plys. Knowing the approximate state of the stress in each ply we could proceed to calculate the failure of each layer. You will recall that we discussed the requirements on the fracture energy with regard to layer and interlaminar fracture. It would now seem only necessary to examine experimentally which of these two energy requirements is appropriate to develop a lower bound for the fracture of a multilayered composite plate containing a through crack.

5. EXPERIMENTAL INVESTIGATION - I

Determination of Elastic Constants

We are now interested in performing experiments which substantiate or reject the postulated failure criterion given by equation (4.8). In an indirect way we shall then examine through experimentation a) whether the assumption that the crack propagation occurs along the fiber direction is indeed valid and b) whether the energy exchange process as the crack advances is as predicted by equation (4.8). In order to evaluate this latter equation and to perform the correlation with the experiments it is first necessary to evaluate the elastic constants E_{xx}, E_{yy}, G_{xy} and γ_{xy}, as well as the fracture energy Γ. In this section we consider the determination of E_{xx}, E_{yy}, G_{xy} and ν_{xy}.

The methods by which we choose to determine these material parameters were three-fold: the moduli E_{xx} and E_{yy} were determined by a) static bending of a cantiliver beam, b) vibration of a cantilever beam, c) uniaxial tension test, x being along the fiber direction and y being perpendicular to this. The constant G_{xy} was determined with the aid of a torsion pendulum. In as much as there was no easy way to determine the parameter ν_{xy}, the sensitivity of the stress distribution to the variation of this parameter was examined. We see from equation (3.14) that the way the Poisson's ratio enters the stress distribution is through the definitions, in equation (3-13), of the constants s_1 and s_2. Upon analysing the dependence of these constants on Poisson's ratio ν_{xy} and using the value, as we shall determine later, of $\frac{E_{xx}}{2G_{xy}}$ approximately 10, we find

that the variation of the constants s_1 and s_2 is approximately 1 % or less as the parameter ν_{xy} take the values from 0. 2 to 0. 4. In view of this relative insensivity of the stress distribution to this parameter we feel that it was not necessary to perform an elaborate experimental analysis of this quantity which is difficult to measure; instead we believe it was adequate for the present purposes that this quantity be estimated from existing analysis such as the rule of mixture given by equation (5.1), (Ref. 8).

$$\gamma_{xy} = V_m \nu_m + V_f \nu_f \qquad (5.1)$$

In choosing a value for ν_f we must be aware of the fact that the fibers by themselves are not isotropic. We therefore choose ν_f as the lateral Poisson contraction of fiber which is subjected to the axial load.

A. Cantilever Beam Test

The determination of the moduli by the beam bending method is very sensitive to errors in the beam thickness. Indeed, since the thickness appears as the third power in the relation between deflection and the elastic moduli as seen from the following equation.

$$E = \frac{K}{\delta} \frac{PL^3}{bt^3} \qquad (5.2)$$

where, E, is elastic modulus; P, is the load; L, length of the cantilever t, the thickness of the beam; b, the width of the beam; δ, is the deflection at the end of the cantilever and K being a numerical constant which takes values of 0. 344 and 1. 25 for the load at the quarter and mid span, respectively. In order to determine this

TABLE 5-1

BEAM BENDING DETERMINATION OF E_{xx}

Loading Point	Load		Deflection		E_{xx} in PSI
	gms.	lbs.	cms.	ins.	
Quarter Span	17.26	0.038	0.48	0.189	13.75×10^6
	27.26	0.0608	0.77	0.303	13.70×10^6
	37.26	0.082	1.05	0.413	13.55×10^6
	47.26	0.104	1.35	0.532	13.40×10^6
	57.26	0.129	1.63	0.642	13.70×10^6
Half Span	17.26	0.038	1.73	0.681	13.9×10^6
	27.26	0.608	2.73	1.075	14.0×10^6
	37.26	0.082	3.72	1.465	13.9×10^6

Length of Cantilever = L = 16"

Width of Cantilever = b = 0.239 ± 0.03"

Thickness = t = (0.044 ± 0.001")

Elastic Modulus = $(13.74 \pm 0.02) \times 10^6$ psi

TABLE 5-2

BEAM BENDING DETERMINATION OF E_{yy}

Loading Point	Load		Deflection		E_{yy} in p. s. i.
	gms.	lbs.	cms.	ins.	
Quarter Span	17.26	0.038	0.38	0.1495	1.435×10^6
	27.26	0.0608	0.59	0.232	1.45×10^6
	27.26	0.052	0.84	0.323	1.44×10^6
Mid Span	17.26	0.038	1.34	0.527	1.45×10^6
	27.26	0.0608	2.27	0.893	1.43×10^6
	37.26	0.082	3.07	1.29	1.42×10^6

Length of Cantilever = 10"

Width of Cantilever = 0.483 ± 0.006"

Thickness of Cantilever= 0.499" ± 0.001"

Elastic Modulus = $(1.435 \pm 0.02)10^6$ psi

thickness reliably and also remove a layer of matrix material deposited on the exterior faces of the beam cut from the manufactured plate, the beam specimens of nominal thickness (0.0564 $\pm$ 0.003) inches and (0.0613 $\pm$ 0.003) inches were ground to the thickness (0.04391 $\pm$ 0.001) inches and (0.04988 $\pm$ 0.001) inches.

The static beam bending test was performed as follows: The beam was clamped between two steel blocks to a heavy and rigid stand. The cantilever was then subjected to the load at the quarter span and mid span as measured from the support. The deflection at the free end of the beam was then measured with a travelling telescope. This permitted the resolution of the deflection to 0.01 cm and since the total deflection measured was of the order of at least 0.5 cm, accuracy was approximately 2%. In tables 5.1 and 5.2 we give the results of load vs deflection relation for this test.

On the basis of the deformation encountered in the beam it was found that the strains in the beam were less than 0.1%. One would therefore conclude that the linear theory of beam bending is satisfactory in the determination of the moduli by this method. The equation (5.2) gives the relation from which E_{xx} and E_{yy} were calculated and their average values were found to be,

$$E_{xx} = 13.74 \times 10^6 \text{ psi}$$

$$E_{yy} = 1.435 \times 10^6 \text{ psi}$$

B. Cantilever Vibration Test

In order to check the results of the cantilever beam test, we performed a cantilever vibration test. The cantilever beam was excited by means of a speaker, the frequency of which was controlled by an

TABLE 5-3

VIBRATION DETERMINATION OF E_{xx}

Span	Mode of vibration	Cycles/sec.	E_{xx} in p.s.i.
	2	96.6	13.60×10^6
12"	3	274.0	13.94×10^6
	4	538.1	14.0×10^6
	5	888.8	13.94×10^6
	1	21.9	* 13.30×10^6
10"	2	144.4	* 14.72×10^6
	3	396.9	14.18×10^6
	4	778.8	14.18×10^6
	5	1284.8	14.18×10^6

Cross-Section of Beam as in Table 5-1

Density of Material = 5.37×10^{-2} lb/in^3

* Denotes elimination in the average

$E_{xx} = (14.02 \pm 0.05) \times 10^6$ psi

TABLE 5-4

VIBRATION DETERMINATION OF E_{yy}

Span	Mode of vibration	Cycles/sec.	E_{xx} in p.s.i.
	2	50.8	* 1.510×10^6
10"	3	139.8	1.465×10^6
	4	274.6	1.465×10^6
	5	454.4	1.465×10^6
	2	78.6	1.465×10^6
8"	3	218.3	* 1.799×10^6
	4	427.4	1.452×10^6
	5	708.4	1.452×10^6

Cross-Section of Beam as in Table 5-2

Density of Material = 5.37×10^{-2} lb/in^3

*Denotes Elimination in the average

$E_{yy} = (1.46 \pm 0.05) 10^6$ psi

oscillator. The first five modes of vibration were determined by increasing the frequency of the speaker continuously from zero. The displacements measured were of the order of 0.01". A capacitance pick-up, which responded sufficiently well to the graphite-epoxy composite, was used to determine the amplitude and the resonance frequencies by examining the amplitude for the first five modes. The experiment were performed for the two lengths, 12" and 10" when E_{xx} was to be determined and for the two lengths, 10" and 8" when E_{yy} was concerned. The specimens used in these measurements were the same as used in the static cantilever test. The data for the vibration tests are given in table 5. 3 and 5. 4. The average values for E_{xx} and E_{yy} as determined by this test are,

$$E_{xx} = 14.02 \times 10^6 \text{ psi}$$

$$E_{yy} = 1.460 \times 10^6 \text{ psi}$$

C. Uniaxial Tension Test

In order to determine the reliability of the above two tests, a third experiment was performed, in which the same specimens as used before were extended in the Instron tester under uniaxial tension. The strain was measured by a clip-on extensometer (Model TTC Instron Number 949) which was calibrated to an accuracy of 0. 5%. The tables 5. 5 and 5. 6 give data of these tests. The values for E_{xx} and E_{yy} obtained in three different tests mentioned above have been summarized in table 5. 9. A systematic discrepancy is apparent from this table. But rather than explain this discrepancy at this point we continue first the description of the tests for the determination of the remaining properties and then return to this question for further discussion.

TABLE 5-5

TENSILE DETERMINATION OF E_{xx}

Load	Extensometer Reading	E_{xx} in psi
lbs.	inches	
434	0.004	15.75×10^6
445	0.004	15.79×10^6
444	0.004	15.78×10^6
435	0.004	15.76×10^6

Gauge of Extensometer = 1.096 inch

Width of Specimen = 0.252 inch

Thickness of Specimen = 0.044 inch

$E_{xx} = (15.77 \pm 0.02)\ 10^6$ psi

TABLE 5-6
TENSILE DETERMINATION OF E_{yy}

Load (lbs)	Extensometer Reading inches	E_{xx} in psi
134	0.0045	1.36×10^6
153	0.0040	1.38×10^6
173	0.0035	1.37×10^6
173	0.0035	1.37×10^6

Gauge of Extensometer	1.085 inch
Width of the Specimen	0.496 inch
Thickness of the Specimen	0.0498 inch

$E_{yy} = (1.37 \pm 0.02)10^6$ psi

Average values of E_{xx} and E_{yy} obtained in the uniaxial tension tests are,

$$E_{xx} = 15.77 \times 10^6 \text{ psi}$$

$$E_{yy} = 1.37 \times 10^6 \text{ psi}$$

D. The Torsion Pendulum Test

Finally we need to determine the inplane shear modulus of the material. In order to do this we note that if we manufacture a strip of material with the fibers running along the strip, the twist-torque relationship of such a strip depends on the required shear modulus. Furthermore, if we use such a strip in a torsional pendulum, then we can determine the required shear modulus by measuring the period of such pendulum. Thus we can use the beam manufactured for the determination of E_{xx} in the beam bending test for this experiment. (Fig. 5.1) shows the details of the experimental arrangement. By choosing the moment of inertia of the disc sufficiently large, so that the period could be determined with the aid of a stop-watch, several repeated measurements were made in which time for 10, 15, 20, 25, oscillations were measured. Then the shear modulus was calculated from the relation,

$$G = \frac{4\pi^2 \ell I}{k\,(2a)^3\,(2b)\,T^2} \tag{5.3}$$

where

T = Period

ℓ = Length of the pendulum

I = Moment of Inertia of Disc

k = Constant depending on the ratio a/b

b = Breadth of specimen

a = thickness of the specimen

TABLE 5-7
DETERMINATION OF G_{xy}

No.	No. of Oscillations	Time Measured in Secs.	Period in Secs.
1	15	13.2	0.88
2	25	22.5	0.90
3	10	9.0	0.90
4	15	13.3	0.89
5	15	13.2	0.88
6	15	13.4	0.895
7	15	13.4	0.895
8	20	17.9	0.895
9	15	13.2	0.88
10	20	17.8	0.89

Average Period = 0.89 secs.

Length of the Pendulum = 15 5/8 inches

Cross-section as in Table = 4.1

$G_{xy} = (0.675 \pm 0.007)\ 10^6$ psi

by using the average value of the period. Table 5.7 gives details of data. The value of G_{xy} thus calculated was,

$$G_{xy} = 0.675 \quad 10^6 \text{ psi}$$

E. Estimation of ν_{xy}

We estimate the value of ν_{xy} by the rule of mixture as mentioned in the beginning of this section. The volume fraction of graphite was determined by first finding the weight fraction of the constituents. By burning away the epoxy material in an oven and weighing the residue weight and the weight of preburnt sample the graphite weight fraction was determined. The weight fraction was 65.9% fiber and 34.1% epoxy. From the densities of these constituents this corresponds to the volume fractions of 59.2% fiber and 40.8% epoxy. See Table 5.8.

The representative values for the γ_{xy} for the fibers, the x axis being along the axis of the fibers, and γ for the matrix was taken from (8) to be 0.2 and 0.35 respectively. The equation (5.1) then gives γ_{xy} for the composite as 0.29.

F. Choice of the Material Properties

In view of the diversity of the experimental results as indicated in table 5.10 we now have to determine which of these values is appropriate and least prone to experimental error for incorporation in our further analysis. First we observe that both the cantilever vibration test and the static cantilever test generate material properties which are in close agreement, i.e., on the average within 3%. However, both the vibration test and static cantilever test show a disparity of approximately 10% with the results of the tension test.

TABLE 5-8
DETERMINATION CONSTITUENT FRACTIONS

Weight of Specimen Before Burning in gms.	Weight of The Specimen After Burning Epoxy in gms.	% of Fiber by weight
1.345	0.893	66.4
1.512	1.010	66.7
1.098	0.715	65.2
1.235	0.805	64.9
1.423	0.945	65.3

Percentage of Fiber by Weight = 65.90

TABLE 5-9
COMPARISON BETWEEN VARIOUS TEST RESULTS

Material Property	Experimental Procedure	Numerical Value
E_{xx} (Along Fibers)	a) Static Cantilever Test	13.74×10^6 psi
	b) Cantilever Vibration Test	14.02×10^6 psi
	c) Uniaxial Tension	15.77×10^6 psi
E_{yy} (Across Fibers)	a) Static Cantilever Test	1.435×10^6 psi
	b) Cantilever Vibration Test	1.46×10^6 psi
	c) Uniaxial Tension	1.37×10^6 psi
G_{xy}	Torsion Pendulum	0.675×10^6 psi
ν_{xy}	Approximate Estimation	0.29
Weight Fraction of Fiber	Burning off the Epoxy	65.9%

Let us first consider the error in the measurement of the thickness of the beam. The thickness measurement was correct to 2%. This gives rise to an error of approximately 6% in the value of the modulus, while in the uniaxial test it is 2%. Thus the uniaxial test is better than the bending test in this respect. Next we note that in the bending test both the tension and the compressive properties are involved. If the tensile and compressive properties should be different, one would then expect that the resulting average modulus will not necessarily be in close agreement with the tension modulus as determined in the uniaxial tension test. Third, if the composite material were to have flaws aligned parallel to the fibers the shear rigidity would be impaired and thus one would observe the beam to be less rigid than a perfectly unflawed specimen. This was observed in the case of the beam axis along the fibers, i.e., measurement of E_{xx}. But it is not true when the fibers were aligned across the beam axis. Possible unbonds parallel to the fibers are really responsible for the inconsistent behaviour, which is difficult to ascertain without further careful experimentation. In view of the fact that we wish to use these material properties in the crack propagation experiment, where the stresses are primarily tensile and more or less uniformly so through the sheet thickness it was decided that the Instron tensile test results be used rather than the cantilever test results.

The torsion pendulum results for the value of G_{xy} were accepted without further investigation primarily because the alternative test of performing inplane shear test is very difficult and too time consuming for a study of this scope.

6. EXPERIMENTAL INVESTIGATION - II

Experiment on the Failure Criterion of the Unidirectional Graphite Fiber Reinforced Epoxy

A. Specimen Design

We have already stated that prior to the preparation of the test specimens, calculations for the stress field were carried out to determine the size of the specimens. The reason for doing this was twofold. First, the material is expensive and for this reason the supply of the material was very limited. It was therefore necessary to make optimum use of the material available to us by making the specimens as small as possible. With this constraint on the specimen design, it was necessary that the size of the specimen was such that the stress distribution encountered in the laboratory experiment did not deviate more than a specified minimum from that which one would have in an infinite sheet, as our analysis assumed.

The size and the shape of the specimen were chosen ultimately by the following procedure. The stresses in an infinitely large sheet were calculated and the rectangular boundaries surrounding the crack were chosen such that the maximum deviation of normal stresses on that boundary did not vary by more than 5% from the stresses at infinity. The boundaries thus chosen were used to cut the specimen from the supplied sheet. Evidently this size will depend on the size of the crack in the sheet. The minimum size of the crack is determined by the irregularities of the microstructure of the material as well as the thickness of the sheet. It was felt that the crack of half-inch length was

sufficient to overshadow the microstructural irregularities as well as the effect due to the finite thickness of the sheet. This characteristic length was used in determining the absolute size of the specimen to meet the above requirement of allowable 5% deviation in the stresses. The variations in the displacements were also examined and were found to vary no more than 3% from the average value.

We chose to manufacture the specimens, in which the crack was oriented parallel to the fibers with the following orientation φ between the fiber axis and the tension axis; $\varphi = 90^{\circ}$, 70°, 50° and 30°. The specimen sizes corresponding to these orientations is given in table 6.1. It is also to be noted that the dimension of the specimens along the tension was increased by 1 inch on either side, to provide room for the tabs to fix to the whiffle-tree, a load distribution device which is discussed later.

The ultimate goal of this experiment is to apply loads to boundaries of the specimen and then to determine, from the initial crack size and from the load at which catastrophic failure occurs, whether the failure criterion given by equation (4.8) is satisfied. In the pursuit of this experimental goal three problems arose.

a) It was necessary to consistently introduce a crack of required length in the specimens without premature failure of the specimens.

b) Determination of the crack length introduced.

c) Application of the uniform boundary loads.

The solutions to these problems will be discussed in this order.

TABLE 6-1

SPECIMEN SIZES

Specimen	φ Degrees	Width inches	Length inches	No. of Specimens
A	90	6	8	2
B	70	5	6	2
C	50	3	5	3
D	30	2	5	3

a) Crack Introduction:

The introduction of crack of controlled length into the fiber reinforced material was first practiced on a glass-fiber reinforced composite which could be produced cheaply in our laboratory. Then it was tried on the scrap material which remained after the specimens had been cut out from the sheet. First a $\frac{1}{16}$ inch diameter hole was drilled through the center of the required crack position, i.e., the center of the specimen. Then the specimen was clamped in a vice, the fibers running at right angles to the vice jaws. It was important to note that the vice was new and had ground grips. The center of the hole was placed $\frac{5}{32}$ inch from the edges of the vice grips; this distance was determined by trial and error. A specially ground steel chisel was placed on the edge of the hole nearest the vice. Upon gently tapping the chisel with a hammer a crack propagated towards the vice grip and because of the elastic vice constraint came to stop approximately $\frac{1}{8}$ inch below the surface of the vice grips. With the experimentation on the scrap material cracks of about $\frac{1}{2}$ inch length could be introduced with good consistency. We were not sure, however, whether the crack introduced by this method deviated enough from $\frac{1}{2}$ inch, which unknown variation might later show up as experimental scatter in the analyzed data.

b. Measurement of the crack length

The examination of the surface of the totally broken specimen revealed that there was no difference between the preformed crack and the surface of the further growth of the crack. In order to deliniate the length of the initial crack it was necessary to introduce

some kind of surface marking which determined the crack front prior to the testing of the specimen. This was accomplished by introducing a dye into the crack which stained the crack surfaces. Following the final testing of the specimen, one was then able to distinguish the surface of the preformed crack from the surface generated during the final test. The dye introduced in the crack consisted of a solution of eosin in methyl alcohol. Eosin is a fluorescent agent which is visible under ultraviolet light. The solution had an advantage over other liquids in that it had low viscosity and its surface tension was sufficient to draw the solution into the crack tip region. It was recognized that the introduction of methyl alcohol into the crack tip region may have deleterious effects on the further performance of the specimen. In order to check whether methyl-alcohol had obvious undesirable side effects on the composite material, pure methyl-alcohol was introduced onto the surface and no apparent interaction between the epoxy and the methyl-alcohol was observed. In addition the marking of the crack surface took place at least a week before the test, thus allowing enough time for the methyl-alcohol to evaporate. The removal of alcohol could not guarantee, of course, that any possible damage done by the alcohol was not permanent and therefore remained even after the alcohol was gone. By measuring the length of the eosin stained region of the broken specimen in an ultraviolet light the crack length was determined. If this is done on both sides of the crack surface, one obtains a rough estimate of the error in the measurement. This error was found to be about $\pm$ 0.03 inch.

c. Further Specimen Preparation and Whiffle Tree

As we have described earlier, we have gone to some care in designing the proper size and shape of the specimen to insure that the stress state is reasonably well approximated by that in an infinite plate. For the isotropic specimen it is customary to clamp the edges of the properly sized specimen and to pull the clamped edges apart, in order to apply approximately uniform tension to the crack perforated sheet. It is a characteristic of the orthotropic plates that, when they are stretched along one of the principle material axes, the deformations are symmetric; however, if the loads are applied such that the tension is at some angle with respect to the fiber direction, both the shear and extension take place. If we therefore persist in applying the loading condition, through clamped edges to an orthotropic material, then the clamped boundary condition will not be able to produce approximate uniform tension. In order to circumvent this undesirable constraint, at least partially, we proceeded with the following method of loading.

Along the boundary, where loads were to be applied, we glued short metal tabs with an epoxy adhesive (ECCOBOND 55 + CATALYST 9). In addition, after the adhesive had set we enlarged the holes through the bond area and inserted bolts which were tightened with nuts to strengthen the joints, which increased the capacity of the joints by 10-15%. As shown in (fig. 6.1) the other end of the glued tabs were perforated by reamed holes of $\frac{1}{8}$ inch diameter, so that a series of tabs protruded from the two loading edges of the plate containing reamed holes. These reamed holes were used for the alignment of the tabs during glueing as described later and to attach the specimen to the

testing machine. Although the tabs were glued directly to the specimen and provided some constraint against the rotation of the edges, it is believed that the situation is not as serious as if a continuous metal strip had been joined to the specimen. We must also comment on the fact that it is the average spacing between the tabs - say the average spacing of the holes through which bolts were inserted - which primarily determines the nonuniformity of the stress field near the edges of the plate. Fig. 6.2 shows the distance at which the knife edge load of value P decays to P/π radial stress in isotropic material and in the orthotropic material under investigation. In a later case the curves in the case of load perpendicular to the fiber as well as for the case of load along the fiber is shown. The decay of stress is inversely proportional to radial distance in all these cases, while the numerical factor is different. When fibers are perpendicular to the load, the decay is faster in orthotropic material, decay being slower in the orthotropic material when the load is along the fiber. In our experiment we were very far from the case of load parallel to the fibers and hence expect the decay comparable to the isotropic case. Without further analysis we believe the transfer of force through the whiffle tree gives reasonably approximate uniform stress distribution at the edge of the specimen.

Let us add one further comment regarding the edge condition on the specimen. According to the calculations referred to earlier, the size of the specimen depended on the orientation of the fibers with respect to the tension axis. Furthermore, the tabs to be glued and bolted to the plate specimen needed to be of a minimum width in order to cope

with the forces to be transmitted to the plate, a limited number of tabs could be attached to the narrower specimens. This minimum number of tabs employed for any of the specimens was four. The constraint on the maximum number of the tabs used was dictated by the maximum space available between the Instron head attachments. The length of the whiffle tree (see fig. 6.3) increases as the number of the tabs is increased. Thus for a maximum of eight tabs, the requirement of both the testing machine size and the size of each tab as dictated by the strength requirement, were conveniently met.

It will be recognized that the glueing of the tabs to the specimen was critical in order to avoid imparting a torque to the tabs during testing which would then shear off the epoxy joints. It was necessary to align the holes which connect the whiffle tree ends and the holes through which the bolts were inserted through the specimen. This was achieved by machining an aluminum plate through which the hole pattern was drilled with a spacing accurate to the nearest 5/1000 inch. The tab holes were reamed. 1/8 inch diameter dowel pins were placed through the holes, and thus the tab joints could be held in the required pattern while curing. The alignment of the tabs as produced by the manner described was approximately ± 2 degrees. The surfaces of the tabs and the specimen were cleaned with methyl-alcohol prior to the application of the adhesive. The epoxy was allowed to cure for eight hours at room temperature before the pins were removed. The tabs were glued on one side at a time and after eight hours of curing the tabs were affixed to the other side. Before testing at least three days elapsed to allow the epoxy to cure thoroughly.

d. Specimen Testing

Although the unidirectionally reinforced graphite-epoxy composite is strong under tensile loads in the direction of the fibers bending strength is relatively low. This fact requires caution in handling. In spite of the care exercised, two of the ten available specimens broke in the specimen preparation process. The specimens were therefore hung from the upper portion of the whiffle tree, after which the other whiffle tree was attached. Also, care was taken that the force be applied in the plane of the specimen since otherwise bending could occur which could be responsible for unpredictable data irregularities.

We used the minimum possible strain rate available in the Instron, corresponding to the 0.02 inch/min. cross head speed. Experiments were conducted at room temperature which was between 68-70^{o}F.

We make note of a small and probably inconsequential accident. Since for the photographic purposes the whiffle tree was not very distinct, it was deemed desirable to spray it with black paint. On the first occasion it is entirely possible that some of the paint may have fallen on the specimen. Whether this has occurred or not was difficult to assert due to the fact that the specimen was black by itself. We believe that although the solvent methyl-alcohol was contained in the paint, we do not think this solvent had any appreciable effect on the specimen; probably most of the alcohol evaporated in the process of

spraying and an insignificant amount of alcohol penetrated into the specimen. In the remaining cases more care was taken not to allow any spray to contaminate the specimen.

7. ANALYSIS OF EXPERIMENT

A. The Calculation of Γ

We consider first the determination of the fracture energy Γ. We recall that it is our aim to determine that combination of the applied boundary stresses σ^{o}_{yy} and σ^{o}_{xy}, for which fracture begins to propagate. The criterion as proposed in equation (4.8) involves five material properties, four of which are determined by the elastic properties viz: E_{xx}, E_{yy}, G_{xy} and ν_{xy}. The fifth is the energy required to generate new surface, which we call here the fracture energy. If equation 4.7 applies to the fracture initiation of a strongly orthotropic solid, then the experimental data such as obtained on the pre-cracked plate and which we have just described, should yield the value of the fracture energy Γ. In table 7.1 we record values of Γ determined from the tests on individual specimens along with the applied stresses σ^{o}_{xy} and σ^{o}_{yy} and other pertinent parameters required to evaluate equation 4.7. In the case of two specimens, special remarks need to be made. In two specimens denoted by C_2 and D in table 7.1 the initial crack length was not of the assigned length inspite of the careful way of introducing the crack as described in section 6. In the specimen C_2 the crack length was too large. The crack length was almost 1 inch long, which was too large for the finite sheet dimension shown in table 6.1. Anticipating the discussion in the next part of this section the failure occurred at a lower stress than would be expected for the infinite sheet. This behavior is reasonable since a larger crack in a finite sheet should produce a larger stress "singularity" than in the infinite sheet. The second specimen for

TABLE 7-1
FRACTURE FAILURE DATA AND RESULTS

Specimen	φ (degrees)	Crack Length (inches)	Thickness (inches	Width (inches)	Failure Load (Lbs)	Γ (lb/inch)	K_I	K_{II}	X	Y
A_1	$90 \pm \frac{1}{4}$	0.579 ± 0.015	0.061 ± 0.002	5.968	672	2.95	983	0	1.04	0.0
A_2	$90 \pm \frac{1}{4}$	0.61 ± 0.015	0.061 ± 0.002	5.875	570	2.23	855	0	0.905	0.0
B_1	$69.5 \pm \frac{3}{4}$	0.579 ± 0.015	0.062 ± 0.002	5.06	635	3.46	980	352	1.035	0.202
B_2	$69.5 \pm \frac{1}{4}$	0.673 ± 0.015	0.060 ± 0.002	5.06	510	2.15	820	300	0.868	0.172
C_1	$49.5 \pm \frac{1}{2}$	0.532 ± 0.015	0.060 ± 0.002	3.06	625	3.44	1010	850	1.055	0.487
* C_2	$49.25 \pm \frac{1}{2}$	0.86 ± 0.015	0.060 ± 0.001	3.06	380	---	772	642	0.815	0.390
C_3	$51.75 \pm \frac{1}{2}$	0.592 ± 0.015	0.061 ± 0.002	3.093	450	2.28	785	660	0.840	0.398
* D	$29 \pm \frac{1}{4}$	0.205 ± 0.015	0.063 ± 0.002	2.06	1280	---	790	1370	0.838	0.790

* Unsuccessful Experiments

which no datum point was obtained, was one with the fiber orientation almost parallel to the direction of the tension. The load obtained in this test was very high. Failure in the specimen occurred at one of the end tabs rather than through the crack. After the specimen was broken artificially it was found that the crack was smaller than 1/2 inch. Since the specimen was designed such that the failure should occur by crack extension, with the tabs holding up under this loading, it turned out that too small a crack made the sheet sufficiently strong so that the failure occurred at one of the tabs, instead of through the crack. Nevertheless we determined the stresses required for crack extension in this specimen, on the basis of maximum fracture energy obtained in the more successful tests. These stresses turned out to be higher than the one, which were produced in the test leading to tab failure. The average fracture energy obtained, disregarding these two points was 2.74 (-20% or +25%) lb / inch.

B. The Failure Interaction Curve

Substitution of the value for the fracture energy into equation 4.8 leads to,

$$\left(\frac{K_I}{945}\right)^2 + \left(\frac{K_{II}}{1745}\right)^2 = 1 \qquad (7.1)$$

If we let $X = \frac{K_I}{945}$ and $Y = \frac{K_{II}}{1745}$ this equation can be written in the form,

$$X^2 + Y^2 = 1 \qquad (7.3)$$

which represents a quadrant of a circle. This quadrant is shown in figure 7.1 along with the points determined in the tests of the individual specimens. We recall that, because of too large a crack in the specimen C_2

and too small a crack in the specimen D the failure points for these cases are inaccurate. The failure of C_2 should have occurred at a higher load if the crack length was smaller, while the failure stress of specimen D was below that value which would have been obtained if failure had occurred through the crack. The arrows show the direction the points should have moved in the case of successful experiments.

C. Error Analysis

We separate the errors in the experiment into two categories, viz: those whose magnitude can be estimated and those for which such an estimation cannot be performed.

Estimable Errors

The errors which can be estimated are as follows:

Elastic properties could be determined as indicated in section to within $\pm$ 2%. The error in the energy calculation due to this is of same order.

The thickness was measured within $\pm$ 3%. However it should be noted that the specimen was manufactured against a cloth surface and the surface was somewhat rough and probably rich in polymer. The error due to the measurement of thickness can be taken into account; however the absolute value of the fracture energy can vary by a greater amount, since the actual thickness of fiber reinforced part of material is somewhat less than that which was measured, because of the rough polymer-rich surface layer.

We estimate that the crack length was measured accurately to $\pm$ 5%.

The measurement of the angle between the direction of tension and the orientation of the crack was accurate to within $\pm$ 2%.

Now let us consider the effect of the above errors on the evaluation of equation 4.7 which we use to determine the fracture energy Γ. Making first order perturbations on the pertinent quantities we obtain for the error in Γ the following equation.

$$\frac{\Delta\Gamma}{\Gamma} = + \frac{\Delta E}{E} - \frac{\Delta t}{t} + \frac{\Delta a}{a} - \frac{4\Delta\varphi}{\varphi} \qquad (7.3)$$

Evaluation of equation 7.3 with the material parameters listed in section -5 results in a maximum relative error in the fracture energy of $\pm$ 25%. The relative error in the two material parameters scaling the ordinate and the absissa in figure 7.1; turns out to be $\pm$ 13%. The error band consistent with these errors is also shown in figure 7.1.

Unestimable Errors

There are several errors which need to be mentioned, but over which we have very little control. As we mentioned earlier the stress distribution near the edge is not actually uniform, but is perturbed with respect to an approximate point load application. Irregularities in the stress field due to the boundary load application will of course depend on the orientation between tension axis and the crack and the fiber orientation and therefore this error will vary from test to test.

We recall that we mentioned in section 6 that we were careful in aligning the plane of the sheet specimen with the tension axis of the Instron. Although we were careful, small amounts of misalignment may have happened. But we do not consider this to be significant.

There is a possibility that the eosin solution did not penetrate completely to the corners of the crack. Repeated tests with scrap material, makes us believe that the error due to this uncertainty is

less than the error in the measurement of the stained crack length by itself.

As we have already mentioned the eosin solution may have affected the material at the crack tip; nevertheless, because of the length of time elapsed between introduction of the eosin solution and the test performance, the alcohol should not be present. The only effect the eosin solution may have had is to cause some permanent damage in the crack tip region.

From the description on the material characterization procedure we recall that the composite material under investigation seems to have different properties under tension and compression. In particular we recall the difference between the results of the beam bending test and uniaxial tension test. This fact may have consequences in the stress distribution of the cracked plate; but, short of a numerical analysis taking this into account, we cannot estimate the magnitude of the error incurred by this material behavior.

D. Final Remarks

We are painfully aware of the fact that the number of successful tests are small. This, it will be recalled, is the result of the limited amount of the expensive material available to us; the second factor was premature failure of some specimens. The following deductions may be made from the previous analysis and ensuing tests.

We found no contradiction to the fact that the cracks propagate parallel to the fibers. For the range of angles between the orientation of the tension axis and the orientation of the crack examined, the

energy criterion of failure is in fair agreement with the test results. Together with the experiments of Wu, including our criticism of his data interpretation, it appears that the energy criterion of failure for advanced composites is a viable proposition.

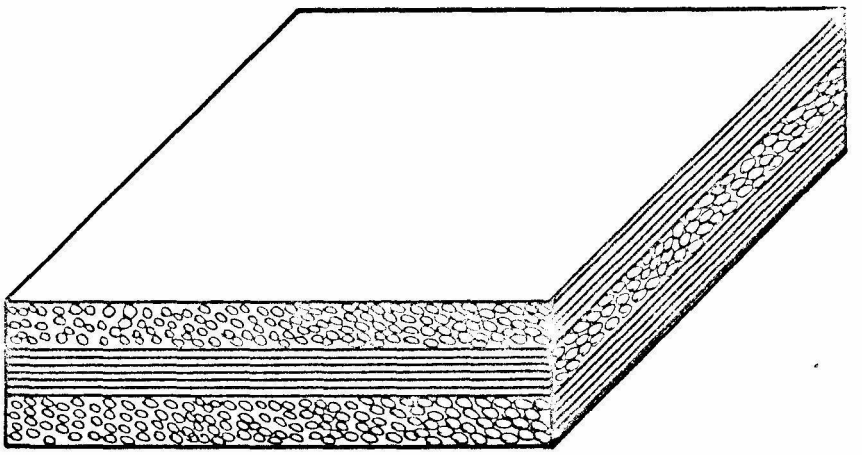

FIG. I.I THREE-PLY MULTIDIRECTIONAL FIBER-COMPOSITE PLYS AT 90 DEGREES

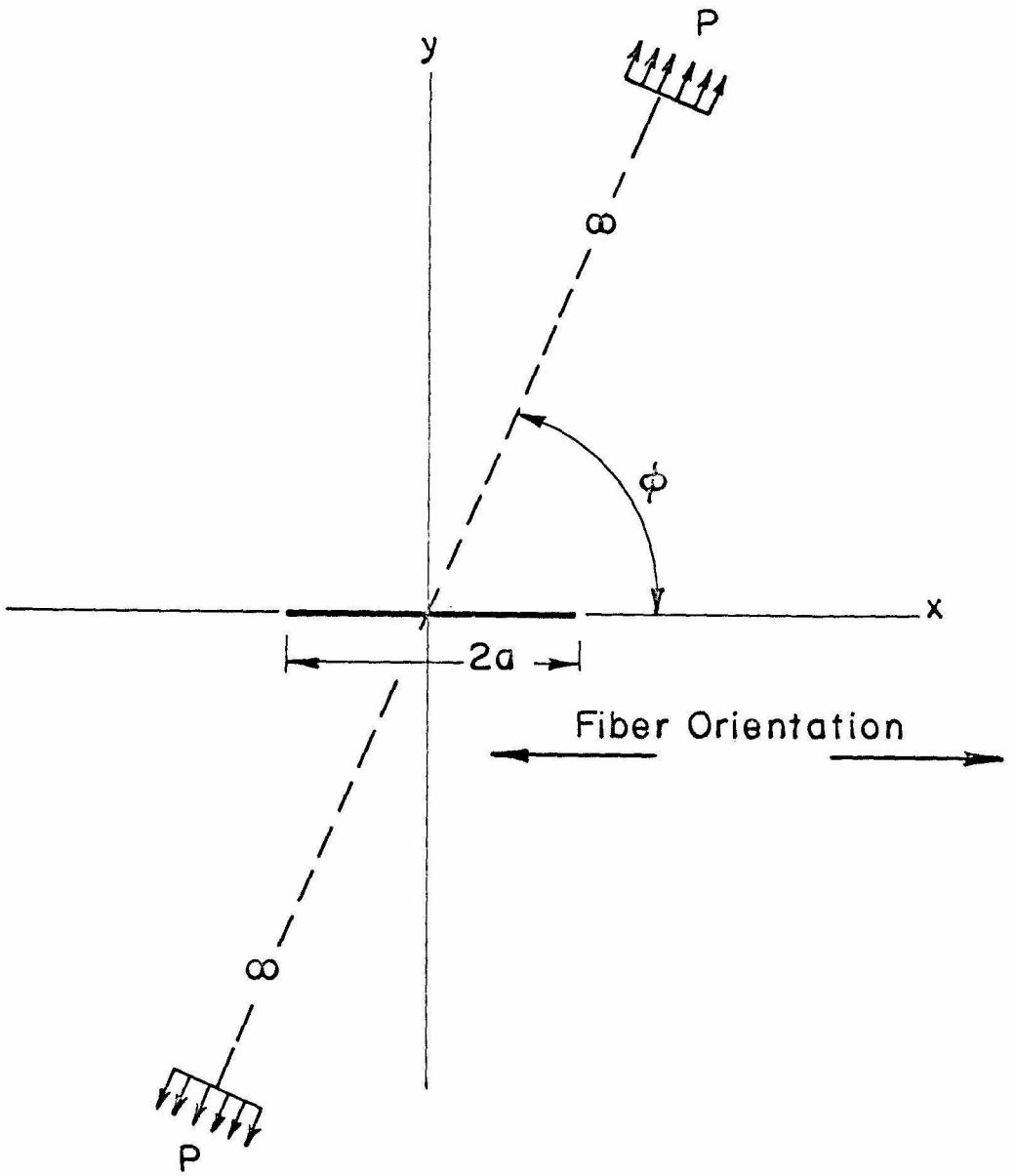

FIG. 2.1 ILLUSTRATION OF THE PROBLEM

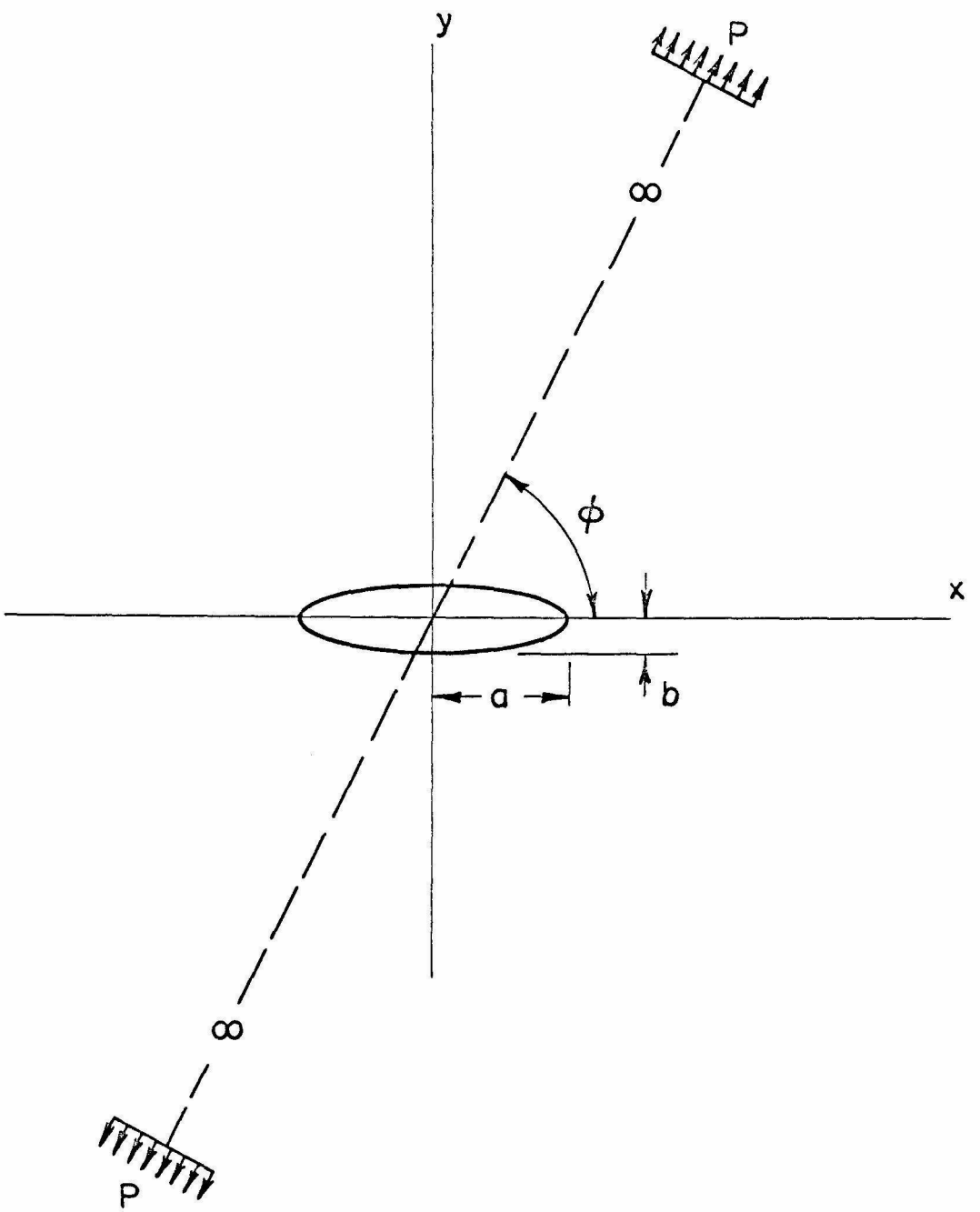

FIG. 3.1

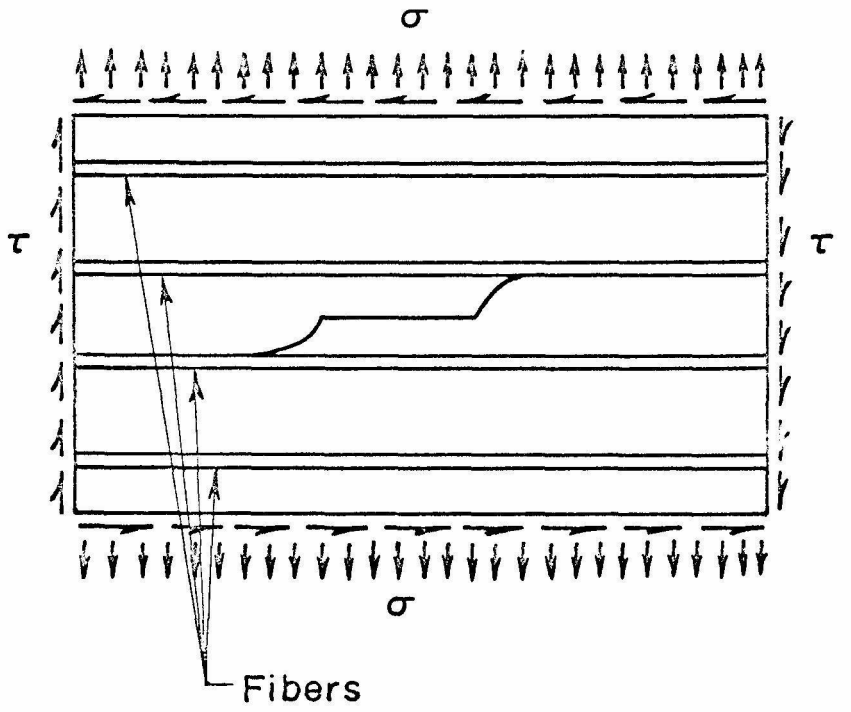

FIG. 4.1 ILLUSTRATION OF QUALITATIVE NATURE OF FRACTURE IN FIBER-REINFORCED-COMPOSITE WITH LOW FIBER CONTENT

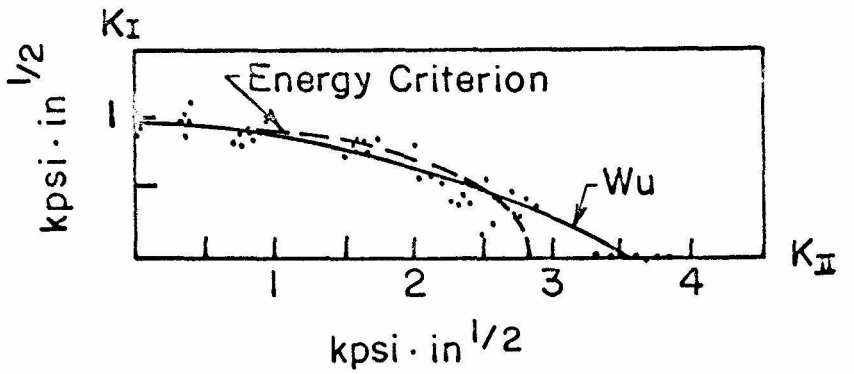

FIG. 4.2 COMPARISON BETWEEN FAILURE RELATION PROPOSED BY WU AND ENERGY CRITERION.

DATA POINTS ARE FROM WU'S EXPERIMENT(6)

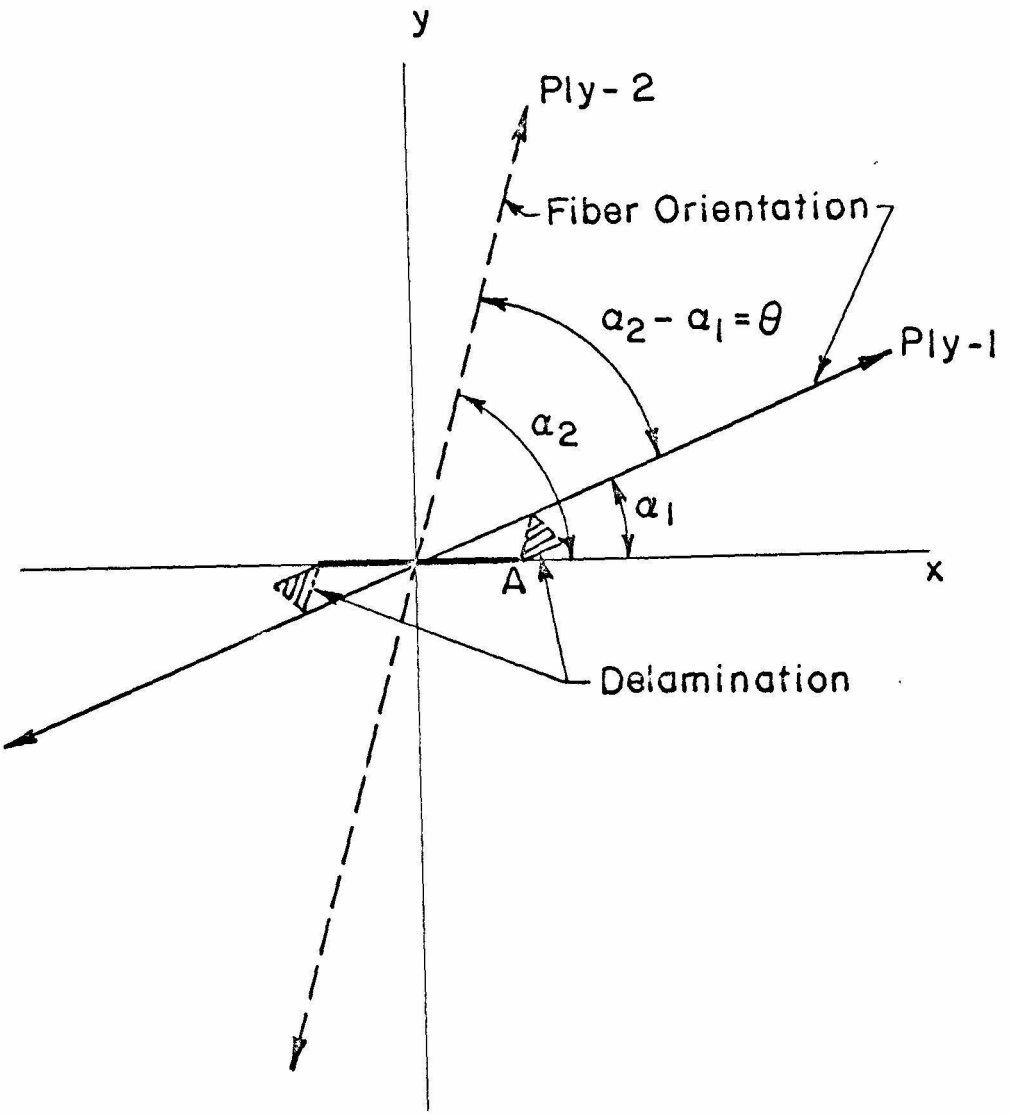

FIG. 4.3 FRACTURE OF TWO-PLY COMPOSITE

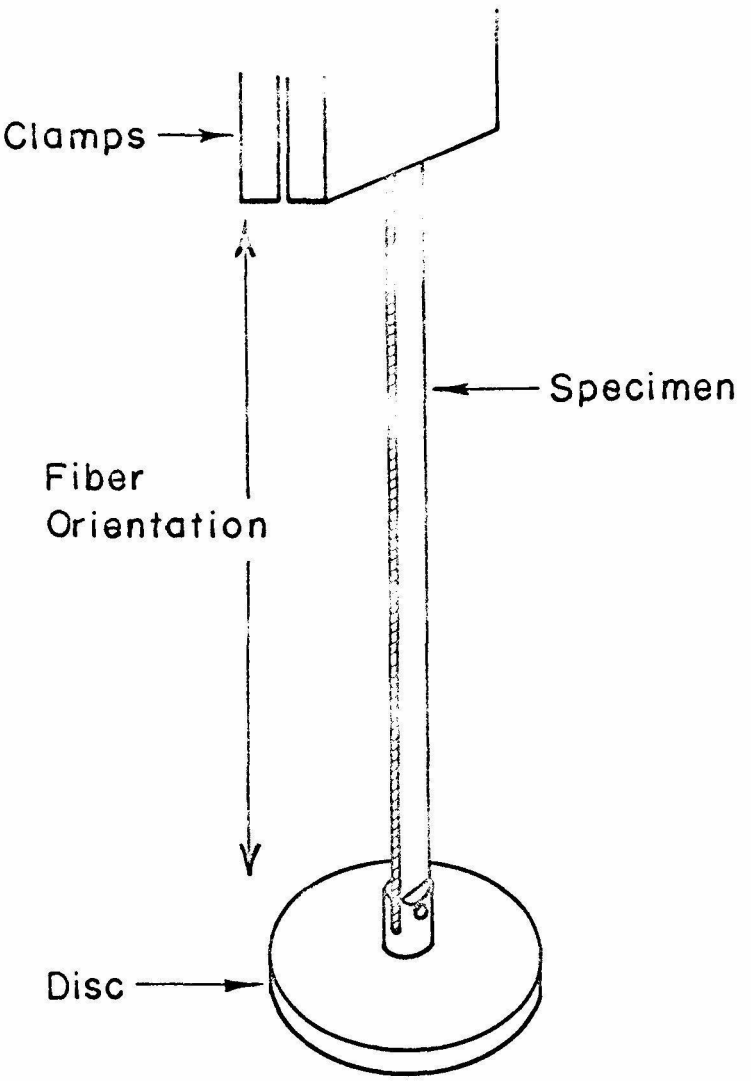

FIG. 5.1 TORSION PENDULUM

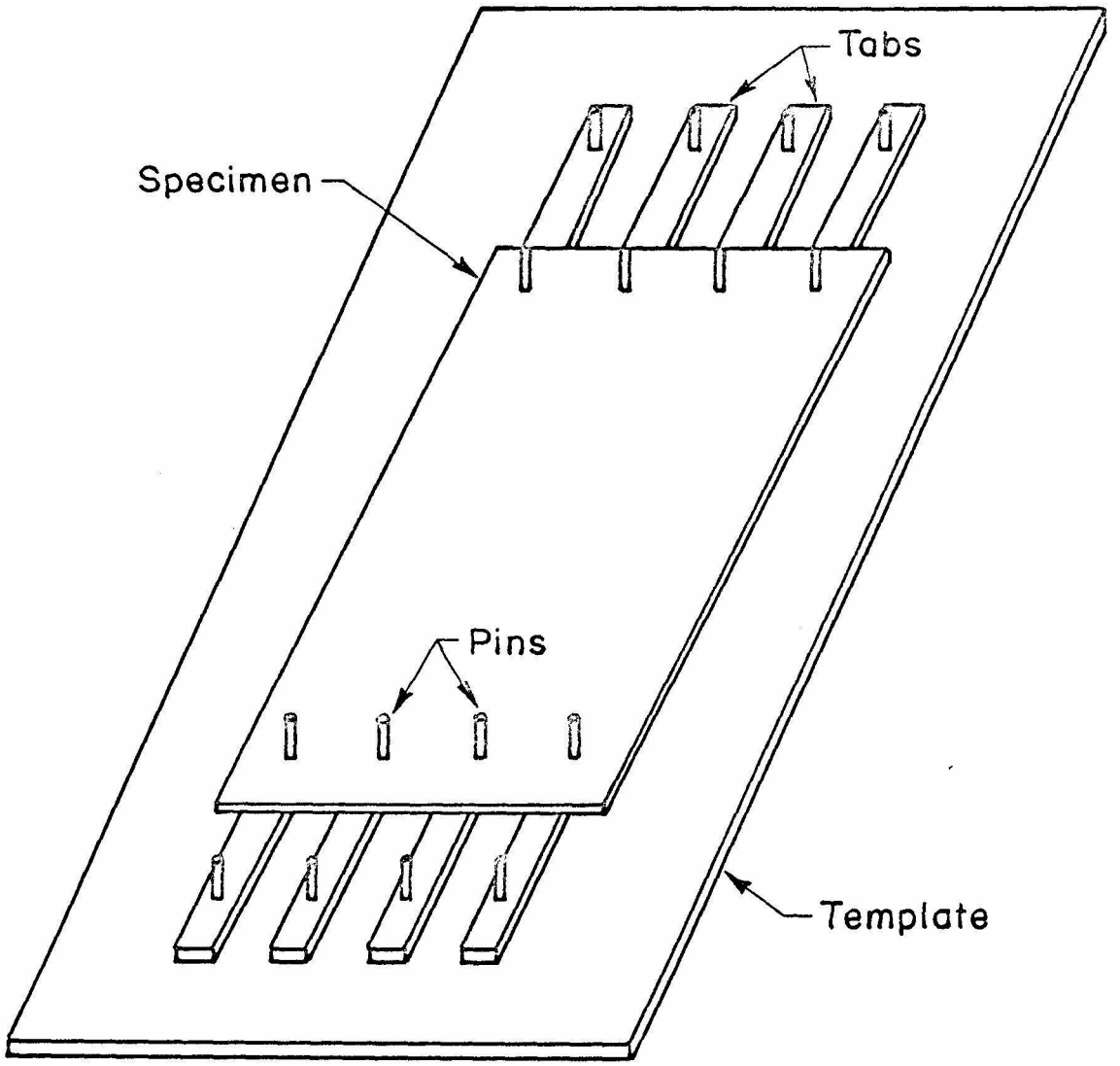

FIG. 6.1 DETAILS OF BONDING

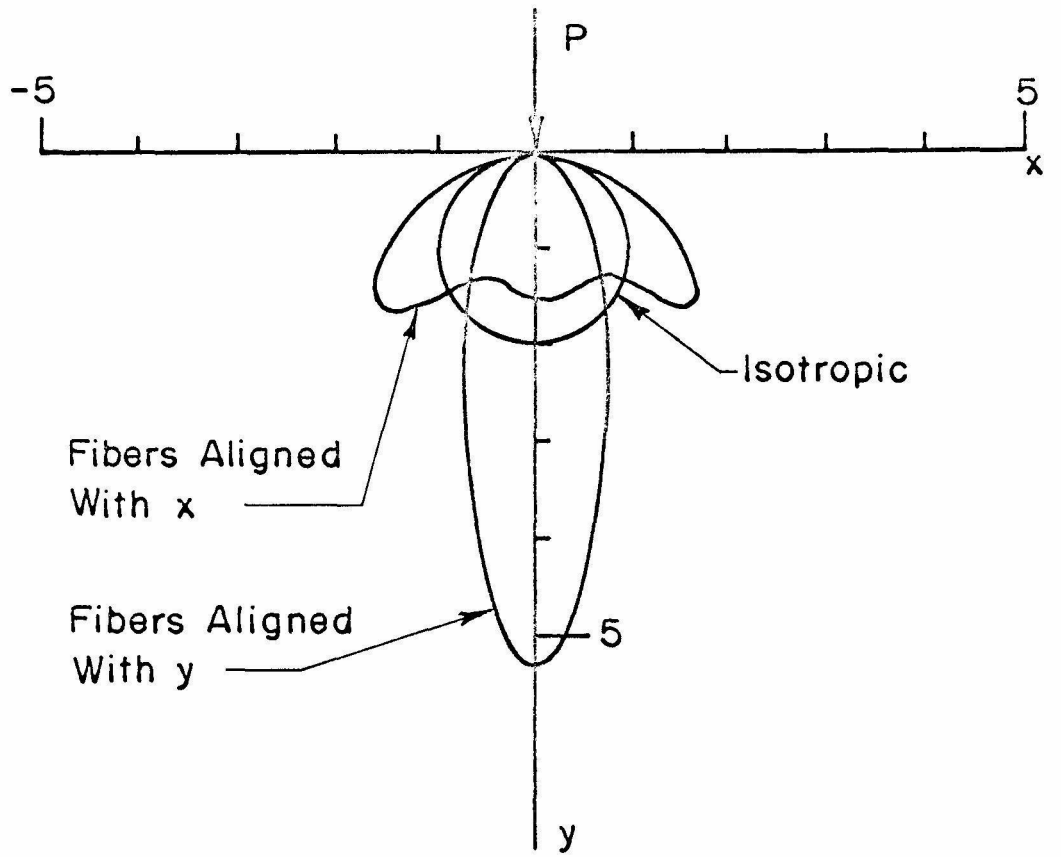

FIG. 6.2 CURVES OF CONSTANT RADIAL STRESS UNDER LINE LOAD ON SEMI-INFINITE MEDIA ($\sigma_{yy} = P/\pi$)

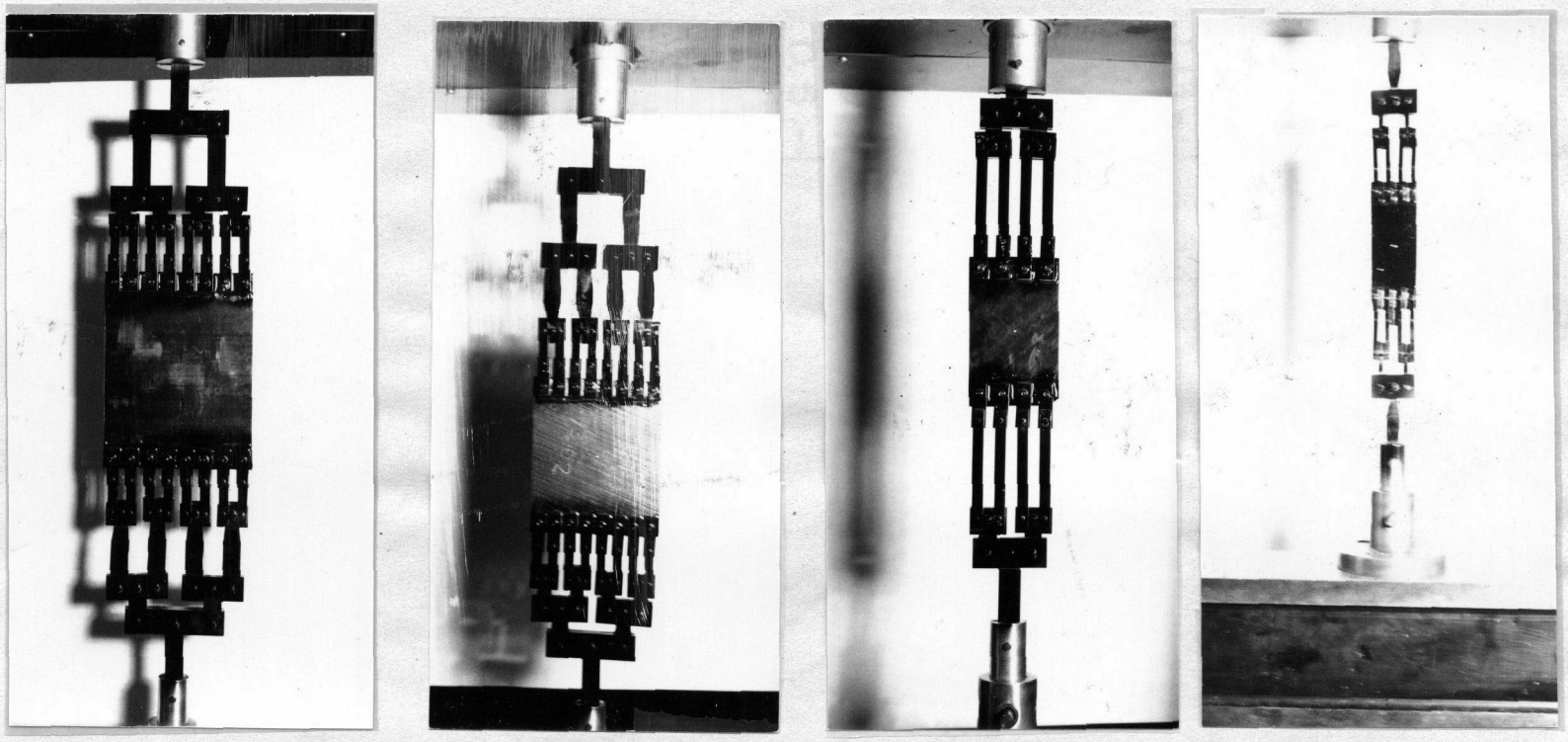

Specimen A Specimen B Specimen C Specimen D

FIG. 6.3 WHIFFLE TREE CONNECTED TO THE SPECIMENS

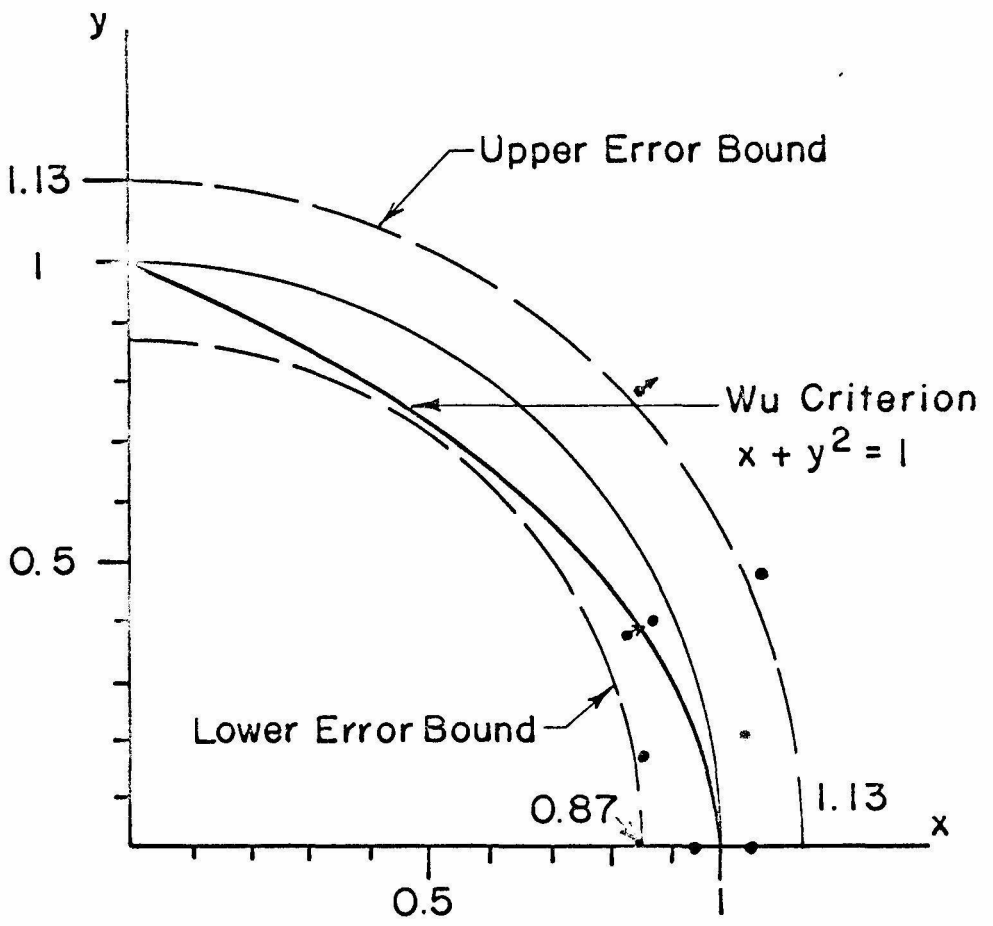

FIG. 7.1 THE FAILURE INTERACTION CURVE

REFERENCES

1. Sanford, R. J. and Stonesiefer, F. R., "Fracture Toughness Measurements in Unidirectional Glass-Reinforced Plastics," J. Comp. Mat., Vol. 5, (April 1971), pp. 241.

2. Tsai, S. W., Halpin, J C., and Pagano, N. J., "Composite Materials Workshop," Technomic Publishing Co., Inc., (1968).

3. Wu, E. M., "Application of Fracture Mechanics to Orthotropic Plates," University of Illinois, TAM 248, (1962).

4. McKinney, J. M., "Mixed-Mode Fracture of Unidirectional Graphite/Epoxy Composite," J. Comp. Mat., Vol. 6, (Jan. 1972), pp. 164.

5. Lekhnitskii, S. G., "Theory of Elasticity of an Anistropic Elastic Body," Holden Day, Inc., San Francisco (1963).

6. Liebowitz, (Editor), "Fracture II," Academic Press (1968).

7. Ashton, J. E., Halpin, J. C., and Petit, P. H., "Primer on Composite Materials: Analysis," Technomic Publishing Co., Inc. (1969).